Rainfall – runoff model of the Huangpu River in Shanghai

Additional Thesis

Fernando Acevedo Goldaracena - 4950798

Supervisors:
Dr. Qian Ke
Dr.ir. Jeremy Bricker
Dr. Hessel Winsemius

November 2019

Abstract

Shanghai is a city located in a coastal region and to understand the flood risks it is exposed to, it is of most importance to first understand the processes that control the water levels for the different flood scenarios. On the downstream regions of the Huangpu river the water level is controlled by the incoming tide, whereas the influence of the discharge generated by rainfall is more clearly identifiable in the water levels of the upstream regions. Historically, the river has reached its highest levels during landfalling typhoon events, which create a combined scenario that involves high sea water levels due to storm surge, and high river water levels consequent not only of the storm surge at the river mouth, but also of the runoff generated by precipitation in the upstream regions. This research project will focus on the later, assessing the impact of torrential rainfall during tropical storms on the water levels along the Huangpu River in the city of Shanghai.

By studying the hydrological regime of the area of interest, three main watershed regions are identified for the Huangpu river basin; the Taihu lake basin situated upstream regulates the yearly discharge on the downstream areas of the river and is controlled by means of a flood gate which remains closed once a certain flood risk is identified, an agricultural area covered in its majority by an interconnected lake system, and the river basin which encompasses the remaining contributing regions to the system. A hydrological model is built for the Huangpu river basin following the rational method, identifying from satellite databases the dominant land cover classes of the region, the hydrological soil group based on the different soil contents, and the average slope around the area based on a digital elevation model. Using the precipitation data from typhoon Fitow, the hydrological model was used to estimate the corresponding discharge time-series from the storm to be used as input on a hydrodynamic model of the Huangpu river.

The hydrodynamic model of the river was built using the D-Flow Flexible Mesh (DFM) software module developed by Deltares, it was used to assess different scenarios of the river system configuration, allowing to understand not only the overall contribution of rainfall-runoff to the river discharge but also the effect of each of the catchments on the river system. The performance of this model, as well as of the hydrological model was observed by comparing the predicted values with the site measurements at two hydrological stations, one midstream at Huangpu Park which highlighted the strong influence of the tide on the water levels for the river sections closer to the sea, and one upstream at Mishidu where the influence of the rainfall runoff to the water levels could be observed. The hydrological model was then validated using the precipitation data from typhoon Haikui, taking the corresponding discharge time-series for it to the DFM river model and comparing the estimated water levels to the actual measurements. Finally the river profile with the maximum water levels along it as predicted by the DFM model was compared to the scenario modelled with no rainfall-runoff discharge and the measured embankment height to understand the contribution to flood risk of the torrential rainfall during tropical storms on the water levels along the Huangpu River.

Content

I Introduction

The city of Shanghai currently hosts an estimated population of over 26 million habitants, making it the most populated city in China and fifth most in the world. This number is expected only to increase due to the city's strong economic growth and establishment as one of the world's leading global financial centres (Wei & Leung, 2005).

Being home to the world's busiest container port (Lauriat, 2019), the city of Shanghai sits on the coastal area of the East China Sea, on the Yangtze River Delta, and flowing through the city is the Huangpu River, which not only is the main shipping and drainage route to the port, but also serves as the main water resource of the population in the area, its water discharge is mainly regulated by Lake Taihu which sits further upstream.

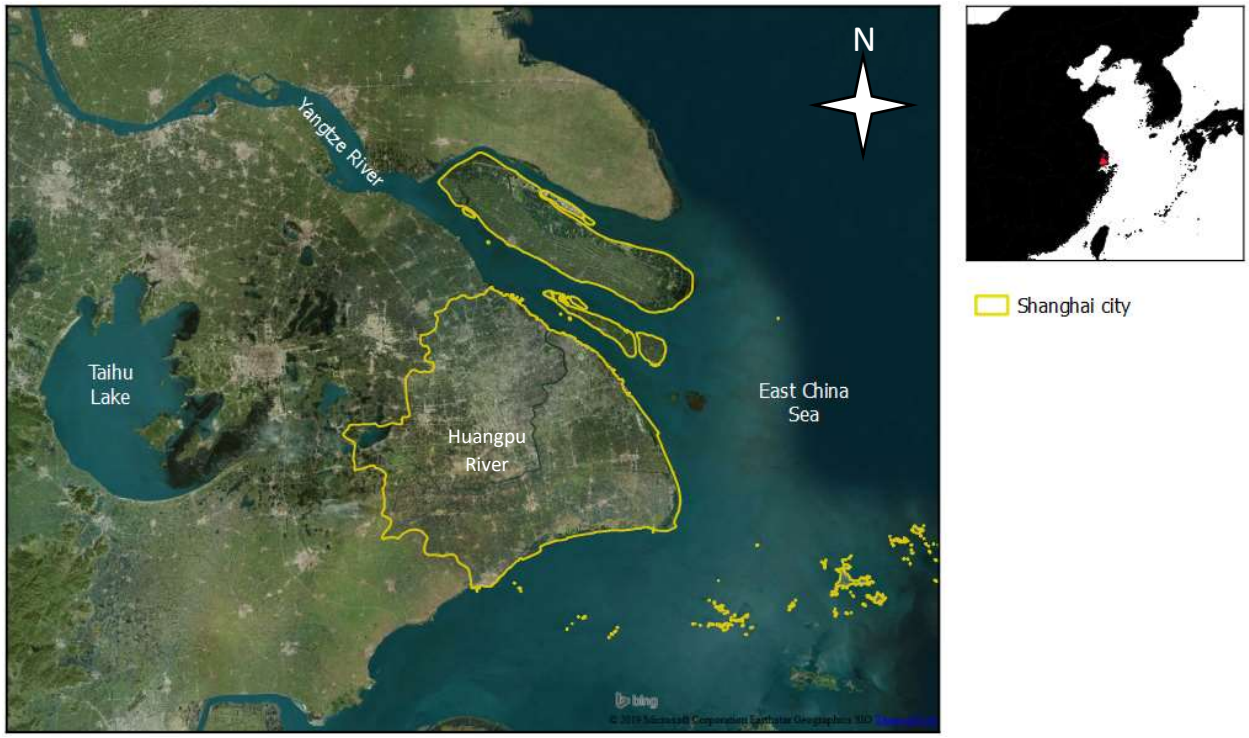

Fig 1. Shanghai city location map and surrounding main water bodies

Considering the proximity of the aforementioned water bodies seen in Figure 1, as well as the generally flat topography of the area, it is easy to understand the exposure to flooding that the city of Shanghai faces, and since both the economic and societal risks to these areas can only be expected to get worse as the potential damages keep increasing, it is important to bring attention to a thorough flood risk assessment of the area.

During tropical storm events mainly three different of flood scenarios should be considered when assessing the total flood risk of the city; storm surges on the East China Sea that endanger the sea dikes of Shanghai, increased water levels in the Huangpu River during torrential rainfall events that threaten the floodwall system, and urban flooding, which due to the increased human activity and urbanization, has only become more likely consequence of a significant reduction in floodwater storage and drainage capacity in the city. As a contribution to the assessment of these three scenarios, this research project will

focus on the second one, by assessing the rainfall contribution to the probability of flooding due to extreme amounts of runoff in the Huangpu River.

I.1 Area of study:

The Huangpu River is located in a subtropical climate zone, with an annual average mild temperature of around 15.8°C, high levels of humidity due to its proximity to the coast, and abundant rainfall during the summer flood season. This coincides with the general occurrence of tropical storms, better known as typhoons in the western North Pacific. These are known to typically occurs between May and November, and even more frequently between the months of July and September. Originating from either the South China Sea, the sea around the Philippine Islands or the sea around Malaysia, they pose as one the biggest threats to the overall safety of the region, especially in the case of landfalling typhoons as they are more closely related to torrential rainfall events than typhoons passing the offshore areas around the coast (Fumin, Gleason & Easterling, 2002). When assessing the risk associated with typhoons, their increased frequency of occurrence and intensity due to global climate change should also be taken into account (Zhang, Liu, Ye & Yeh, 2017).

In total the Huangpu River is 113 kilometres long, with an average depth between 5 and 15 metres and a width between 300 and 500 metres. Upstream, the discharge is mostly controlled by the water stored in Taihu lake and is regulated by means of a flood control gate. The river flows through an area with a rather flat topography surrounded by a series of wetlands and small lakes until it reaches the city of Shanghai (Zhang et al., 2017). Once it reaches the city, the river stretches through a rather complicated water network with many creeks and small drainage canals (Ke et al., 2018), until it finally discharges into the Yangtze River estuary as its final tributary. This means that the river also has a dominant tidal character (semi-diurnal tides), and that the greatest flood risks in the area are presented when the typhoon storm surge coincides with astronomical high tide (Zhang et al., 2017).

River embankments were built along the Huangpu River around the 1950s as a flood defence measure, but because of the increasing water levels due to land subsidence and rising sea levels, they need to be raised periodically to meet with the approved safety standard in 1985 of a 1000 year design return period, which of course is unsustainable, detrimental to the urban landscape and leads to higher potential damages should they ever fail (Zhang et al., 2017).

While the largest percentage of area in the region is covered by cultivated land, this percentage is steadily decreasing with the fast progress of urbanization. Hydrologically, this means that its storage capacity is reducing as its impervious area expands, which in turn leads to an increase in the runoff coefficient and a shortened time of concentration, making the area more susceptible to flooding due to increasing stormwater runoff (Zhou, Liu, Zhong & Cai, 2017). This is further proven by the fact that the historically highest water levels along the river have been encountered on the past 25 years (Ke et al., 2018). Identifying the different land cover types around the region is important when building a hydrological model, as each of the types also has a different transpiration capacity, which is considered to be one of the most difficult components of the water cycle to estimate accurately because of the numerous factors that control it, such as climate, plant biophysics, soil properties and topography among others (Liu et al., 2013).

I.2 Previous studies:

Flooding disasters usually occur due to a combination of different events, in the coastal city of Shanghai the ones to consider are the storm surges caused by typhoon winds, the high water levels in the Huangpu River due to the coincidence of sustained rainfall and high tide, and urban flooding consequence of extreme storms of typical short durations but great intensities. A study in flood vulnerability index for coastal cities in 2012 ranked Shanghai as the most vulnerable to coastal floods worldwide (Zhou et al., 2017). This has led to extensive studies assessing the flood safety of the region as well as different safety measures.

Amongst the most relevant for this research project, (Ke et al., 2018) aimed to evaluate the level of protection of the floodwall system along the Huangpu River by deriving a new series of flood frequency curves, analysing annual maximum levels for the period of 1912-2013 at three stations along the river and determining the best-fit curves with different statistical performance indicators, finding that the current design water levels correspond to exceedance probabilities of 1/500 per year at the stations nearest to the mouth of the river, and of 1/50 per year at the most inland station, all of which are not within the established safety standard of 1/1000 per year, warning also that the neglection of rainfall in the model caused it to underestimate the water levels at the upstream inland station and that its protection levels might be even lower than 1/50 per year, finally suggesting that the influence of torrential rainfall and high runoff as well as the hydrological interactions between Tai Lake and the branches of the Huangpu River should be further analysed particularly for this station, as the results in the more downstream others were mostly dominated by storm tide.

Also assessing the flooding risks of the region (Yin, Yu, Yin, Wang & Xu, 2012) used a coupled flood inundation model to quantify the potential hazards of the different flood scenarios in the Huangpu River floodplain, finding that significant damages occurred mostly during the co-occurrence of typhoon-induced storm surges and astronomical high tides, and that the most susceptible areas to flooding are located within 1-2 km of the river banks.

Building a hydrological model of the Lake Taihu basin (Zhang et al., 2017) assessed benefits of the construction of an estuary gate 5-6 km from the Huangpu River mouth by considering different gate operation scenarios, through a numerical model composed of a hydrological part to simulate runoff generation and routing, and a hydraulic part to simulate channel flows. It was concluded that regardless of the scenario, the gate is helpful for evacuating floodwaters from Lake Taihu to the Yangtze River, reducing both peak values and duration of high-water levels in the lake.

Analysing the effect of typhoons in the entirety of the Chinese country, (Yang, Wang, Li & Gao, 2019) studied the validity of the stationarity assumption for the rainfall record across over 1112 hydrological stations all around China. Among the conclusions, it was found that for the south-eastern coast of the country more than 50% of the flood peaks are caused to tropical cyclones, even though typhoons are not as frequent as in the southern coast where floods are more closely related to monsoon-related extreme rainfall events.

Complementing one of the potential flooding scenarios of Shanghai city (Lyu, Shen, Yang & Yin, 2019) evaluated the urban inundation risks of the metro system in Shanghai over different rainfall return period scenarios, exemplifying the increasing risks of urban flooding in the city as a cause of rapid urbanization

and insufficient drainage capacity, emphasizing the need for flooding adaptation measures to mitigate the extent of the potential catastrophic damages caused by urban flooding.

Of interest when taking into account the different factors involved when building a hydrological model, (Liu et al., 2013) looked to simulate and analyse the changes in daily evapo-transpiration (ET) and water cycle in China for the period from 2000 to 2010 using satellite data, successfully using MODIS land cover data along with the Penman-Monteith equation to estimate both transpiration and evaporation around the country, finding an average annual value of 552 mm for ET in the Yangtze River Basin and a slightly lower value between 300 and 500 mm for the Shanghai region.

I.3 Objective and methodology:

The objective of this research project will be to investigate how the torrential rainfall in the Huangpu River basin caused by landfalling typhoons contributes to the total probability of flooding of the city of Shanghai. This will be done by building a hydrological model of the region to estimate the rainfall contribution to the water discharge in the Huangpu River and then performing a statistical analysis to assess the probability of flooding related to it.

The first step will be to analyse the site topography obtained from the Multi-Error-Removed Improved-Terrain (MERIT) satellite datasets, using QGIS to delineate the main sources of rainfall water to the Huangpu river. Three main catchments as seen in Figure 2 are identified: The Lake Taihu basin, the Dianshan lake basin that encompasses an area covered mostly by water bodies in an interconnected lake system, and the Huangpu river basin with its corresponding tributaries.

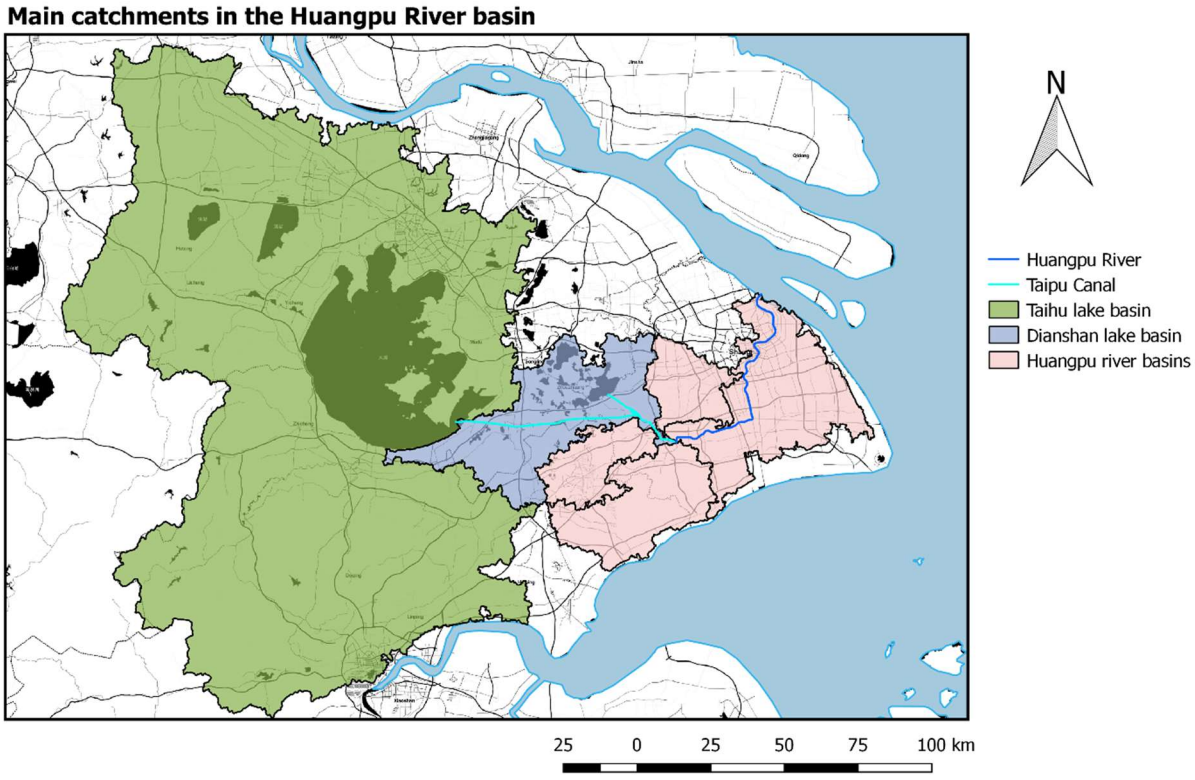

Fig. 2 Main catchments in the Huangpu River basin

Since the outlet of Lake Taihu to the Taipu Canal is regulated by means of a flood gate, it will be assumed that it remains closed throughout the duration of the storm as it is normally during high risk flood events, meaning that the rainfall contribution to this basin will not be taken into account. However, the discharge measurements throughout the period before the storm commences will be used as part of the boundary conditions for a river model. The other basins contributing to the Huangpu river will be divided further into smaller sub-basins with similar characteristics, each of them will be analysed to find a suiting method that describes their hydrological regime.

The period of interest is during typhoon events where the overall probability of flooding is at its largest, the hydrological model will be calibrated with the data recorded during typhoon Fitow, which made landfall in the southern region of Shanghai in October 2013, causing torrential rainfall up to 300 mm/day (Bao et al., 2015) and consequently leading to the highest historically recorded water levels in the upstream locations of the Huangpu river. The resulting water level from this rainfall event will be modelled using a hydrodynamic model of the river created with D-Flow Flexible Mesh model tool, which will allow to assess and compare different rainfall scenarios by estimating the resulting water levels in the different points of interest. These will then be compared to recorded historical water levels and the impact of rainfall events to the probability of flooding will be assessed.

II. Method

II.1 Watershed delimitation

To be able to understand the hydrological processes that dominate the region of study during storm events, the relative elevation of the area was analyzed using the Digital Elevation Model (DEM) from MERIT in combination with the tools offered by QGIS – GRASS, with which the areas of the contributing watersheds to the Huangpu river at different key locations were outlined.

Dataset	Source	Resolution
Digital elevation model Drainage direction Flow accumulation	MERIT	3 arc second

Table 1. Datasets used for watersheds delimitation

The MERIT (Multi-Error-Removed Improved-Terrain) DEM datasets represent the terrain elevations at a 3 second resolution, and were developed by removing multiple error components, such as absolute bias, stripe noise, speckle noise, and tree height bias from existing spaceborne DEMs (SRTM3 v2.1 and AW3D-30m v1), all of which allowed for a significant improvement in data accuracy particularly for flat regions (Yamazaki et al., 2017).

From this DEM dataset, along with water body datasets (G1WBM, GSWO, and OpenStreetMap), high-resolution raster hydrography maps were derived, of particular usefulness for this research project were the drainage direction and flow accumulation maps. The first of these represents the direction of the flow on each particular raster cell according to relative elevation when compared to the 8 adjacent ones, whereas the later estimates the total accumulated flow for each cell depending on the flow direction of the preceding cells.

With the aforementioned maps, by defining the coordinates of an outlet point in QGIS - GRASS it is possible to outline the area inside which all rainfall is collected and drained through this common point, in other words, it allows for the delimitation of the corresponding watershed to that outlet point (Kwast, Menke & Sherman, 2019). Initially, three outlet points of interest are defined; at the mouth of the Huangpu river to identify the total contributing area to this river, of particular relevance to this research project at the point of confluence of all major tributaries to the river to understand the areas that regulate its hydrological regime during tropical storms, and at the outlet of Taihu lake where the outgoing discharge is regulated by means of a flood control gate, this is represented in Figure 2 of the previous section. Later, the sub-basins for the main tributaries to the Huangpu river were found as well in an effort to get a better understanding of the dominant hydrological processes in each of them, these sub-basins are presented in Figure 3.

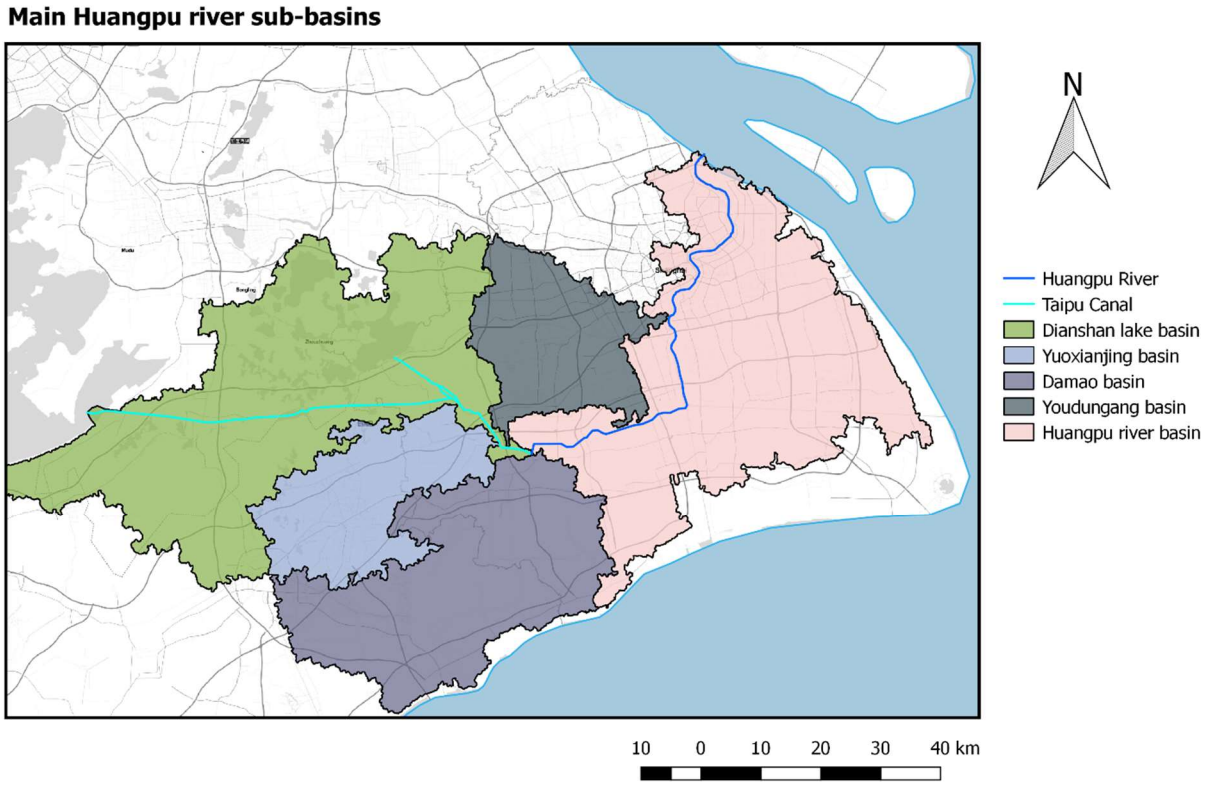

Fig. 3 Main Huangpu river sub-basins.

From Figure 3 four watersheds can be identified from the tributary streams to the Huangpu river, each of them have been assigned the name of its most downstream branch before they join the river's main channel. For a basic understanding of the processes involved in each of the areas, their relative elevation as obtained from the MERIT DEM dataset was analyzed in Figure 4.

The Dianshan lake watershed (top-left) is characterized by large series of wetlands and water bodies, which considerably complicates the analysis the hydrological regime in this particular watershed, as water that falls in this area will not naturally flow directly to certain water outlet, but rather into these water bodies where it will be stored until a certain maximum storage capacity for each of the bodies is reached. Additionally, it is clear that the runoff from this region is regulated by the outflow from both the Taihu lake and the Dianshan lake, the first is regulated by means of a water gate that controls the lake's discharge into the river, whereas the later has two water outlets; the main one at the south of the lake which flows directly into the Taipu canal with around 83% of the total water output, and a second one east of the lake which flows across the Youdungang basin and then directly into the Huangpu River with 17% of the total water output (Xiong et al., 2017).

From this that two scenarios can be considered to understand the impact of rainfall in this region to the total runoff along the Huangpu river, the first will assume that the water bodies are allowed to fill up and eventually inundate their floodplains, preventing any additional discharge of going into the river other than the direct runoff from Dianshan lake, the second scenario will assume that all the rainfall that falls into the water bodies is pumped out into the river, generating the maximum possible contribution of

rainfall to the river discharge. However, this is not the case for the upstream watersheds (Yuoxianjing, Damao and Youdungang) as highlighted by Figure 4, their topography suggests that their hydrological behavior might be closer to that of a conventional watershed, which also means that a more conventional approach towards modelling these areas can be taken, which doesn't happen on the Huangpu river basin where its majority is covered by urban areas and a complex city water network.

To make the most of the available data, the rational method was chosen to model the maximum discharge generated during a rainfall event. Given that the effect of rainfall in the river's water level is more dominant in the upstream region, rather than in the downstream regions where the tide is the dominant process, typhoon Fitow was selected for modelling purposes, as it was during this particular tropical storm when the historical maximum water levels were recorded in the upstream locations of the Huangpu river.

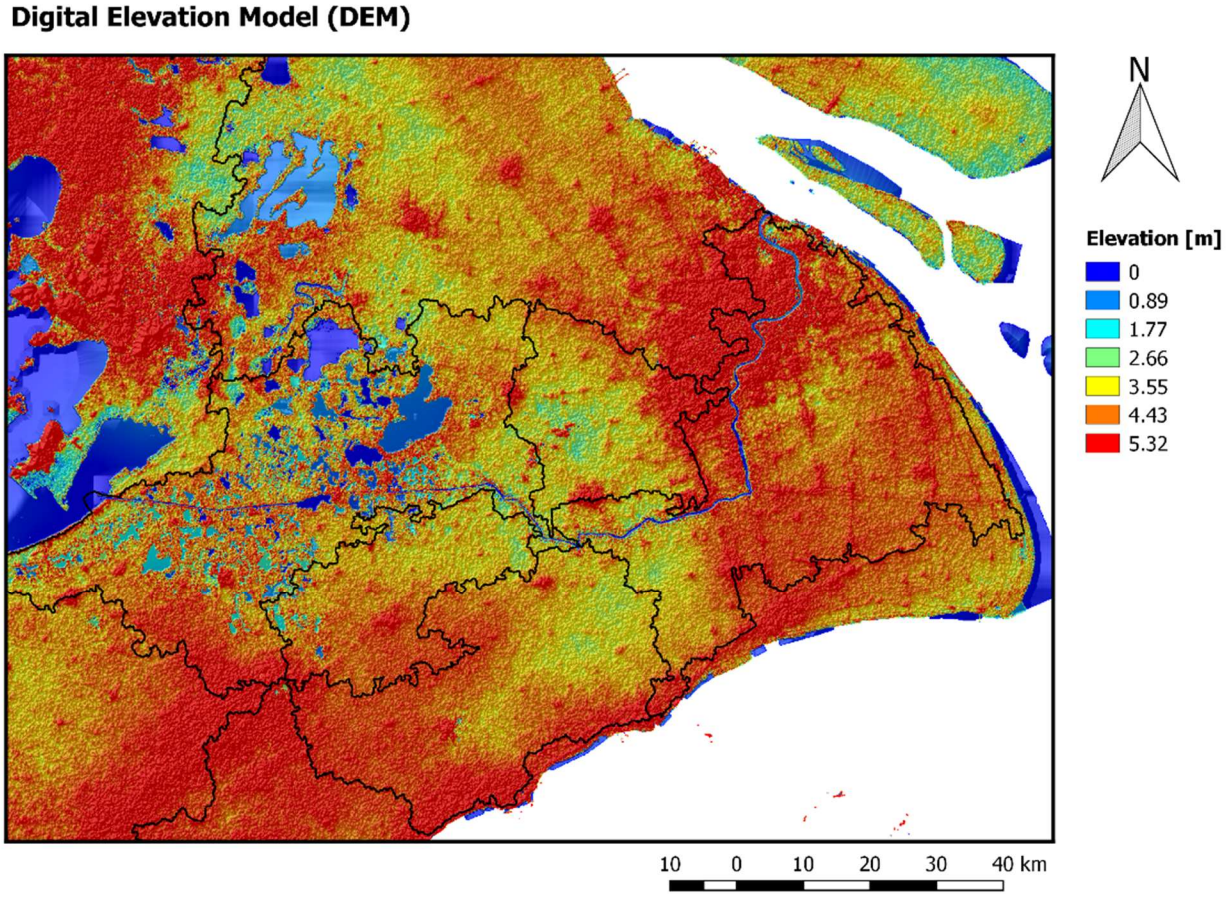

Fig 4. Digital Elevation Model

Finally, Figure 5 provides a more graphical representation of the water system surrounding Shanghai city as well as key locations of water gates and hydrological stations that are later considered for the river model simulations, in this Figure the particular behavior of the complex water network in the Huangpu river basin can also be understood, as the main streams in it on the south and eastern parts of the city are directed outwards towards the coast and not into the river. Table 2 presents then the defined watersheds in the context of this figure.

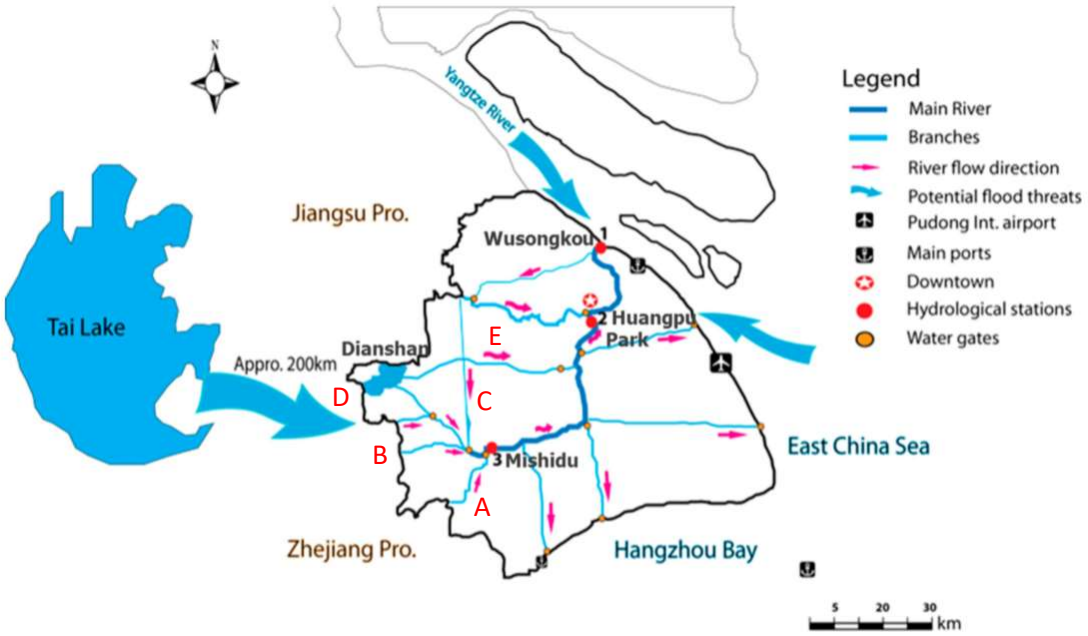

Fig 5. Water system of Shanghai (Ke et al., 2018)

Watershed	In Figure	Regulating water gate	Gate location
Damao	A	Gate A	South of Mishidu station
Yuoxianjing	B	Gate B	At junction of B, C and D tributaries
Youdungang (south)	C	Gate B	
Dianshan lake (south) + Taihu lake	D	Gate C and Gate B	At junction of lake tributaries
Dianshan lake (east) + Youdungang (east)	E	Gate D	Southwest of Huangpu Park station

Table 2. Watersheds and corresponding water gates.

II.2 Rational method

The rational method is a simplistic way to estimate peak runoff rate for watersheds, it uses an empirical formula that relates peak discharge Q [m^3/s], to drainage area A [km^2], rainfall intensity i [mm/hr], a constant $k = 0.278$ for unit conversion, and a dimensionless runoff coefficient C.

$$Q = kCiA$$

Although originally derived for small watersheds, this method has been used in rainfall-runoff analyses since its introduction in 1889 (Mihalik, Levine & Amatya, 2008). It is significantly useful for this research project as it will allow to encompass the gathered information of the area of study to provide a reasonable estimate for the resulting discharge peak and time series during the rainfall event under study (typhoon Fitow) for each of the tributaries to the Huangpu river. The rational method provides better results when storage effects can be neglected (MSMA, 2000), which highlights the reason of not using it for the Dianshan lake sub-basin, where ponding of the stormwater is found across the majority of the region.

To tackle the uncertainty brought by the size of the catchments, these will be further divided in 5 smaller catchments and each will be studied separately. This will also allow for a better estimation of the resulting discharge time series from the rainfall event. This was done with the datasets described in the previous sections and the resulting maps for the Yuoxianjing and Damao sub-basins are presented in Figure 6.

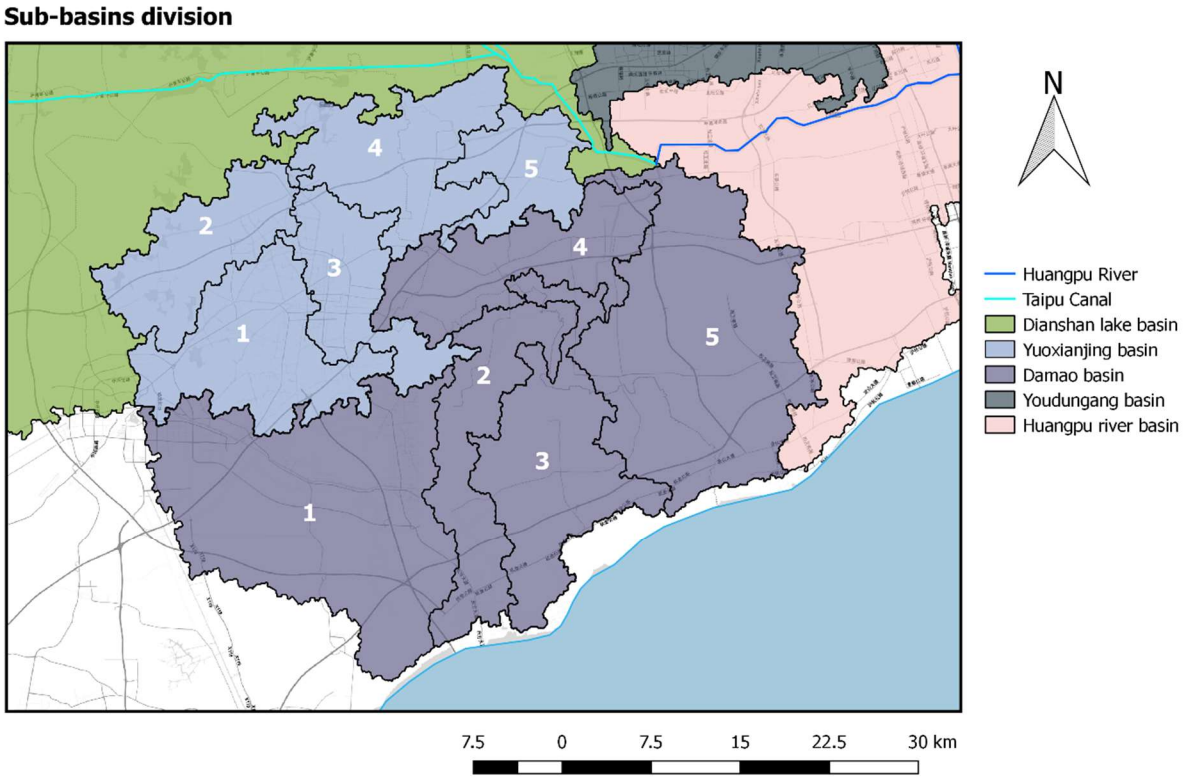

Fig. 6 Graphical representation of the division made to the Yuoxianjing and Damao catchments

II.2.1 Runoff coefficient

To estimate the runoff coefficient for each of the catchments the Table 3 gathers the results found from literature as described by (Liu et al., 2014) was used. From it, that the datasets needed to properly estimate a runoff coefficient for the area were derived, the ones used for the purpose of this research project are described in Table 4.

Land use	Slope (%)	Sand	Loamy sand	Sandy loam	Loam	Silt loam	Silt	Sandy clay loam	Clay loam	Silty clay loam	Sandy clay	Silty clay	Clay
Forest	<0,5	0.03	0.07	0.10	0.13	0.17	0.20	0.23	0.27	0.30	0.33	0.37	0.40
	0,5-5	0.07	0.11	0.14	0.17	0.21	0.24	0.27	0.31	0.34	0.37	0.41	0.44
	5-10	0.13	0.17	0.20	0.23	0.27	0.30	0.33	0.37	0.40	0.43	0.47	0.50
	>10	0.25	0.29	0.32	0.35	0.39	0.42	0.45	0.49	0.52	0.55	0.59	0.62
Grass	<0,5	0.13	0.17	0.20	0.23	0.27	0.30	0.33	0.37	0.40	0.43	0.47	0.50
	0,5-5	0.17	0.21	0.24	0.27	0.31	0.34	0.37	0.41	0.44	0.47	0.51	0.54
	5-10	0.23	0.27	0.30	0.33	0.37	0.40	0.43	0.47	0.50	0.53	0.57	0.60
	>10	0.35	0.39	0.42	0.45	0.49	0.52	0.55	0.59	0.62	0.65	0.69	0.72
Crop	<0,5	0.23	0.27	0.30	0.33	0.37	0.40	0.43	0.47	0.50	0.53	0.57	0.60
	0,5-5	0.27	0.31	0.34	0.37	0.41	0.44	0.47	0.51	0.54	0.57	0.61	0.64
	5-10	0.33	0.37	0.40	0.43	0.47	0.50	0.53	0.57	0.60	0.63	0.67	0.70
	>10	0.45	0.49	0.52	0.55	0.59	0.62	0.65	0.69	0.72	0.75	0.79	0.82
Bare soil	<0,5	0.33	0.37	0.40	0.43	0.47	0.50	0.53	0.57	0.60	0.63	0.67	0.70
	0,5-5	0.37	0.41	0.44	0.47	0.51	0.54	0.57	0.61	0.64	0.67	0.71	0.74
	5-10	0.43	0.47	0.50	0.53	0.57	0.60	0.63	0.67	0.70	0.73	0.77	0.80
	>10	0.55	0.59	0.62	0.65	0.69	0.72	0.75	0.79	0.82	0.85	0.89	0.92
IMP		1.00	1.00	1.00	1.00	1.00	1.00	1.00	1.00	1.00	1.00	1.00	1.00

Table 3. Potential runoff coefficients for different land use, soil type and slope (Liu et al., 2014)

Dataset	Source	Resolution
Digital Elevation Model	MERIT	3 arc second
Land Cover type	USGS – MODIS	500 meters
Soil content maps	ISRIC	250 meters

Table 4. Datasets used for the estimation of the runoff coefficients

The average slope of each cell can be directly calculated from the MERIT DEM dataset with the tools available from QGIS, presented in Figure 7. As expected from the general topographic description of the area, the slope is very mild along the catchment, which will translate to low runoff coefficients as well as large times of concentration. This map also highlights the unique complexity of the upstream catchment, in which ponding is clearly the dominant process.

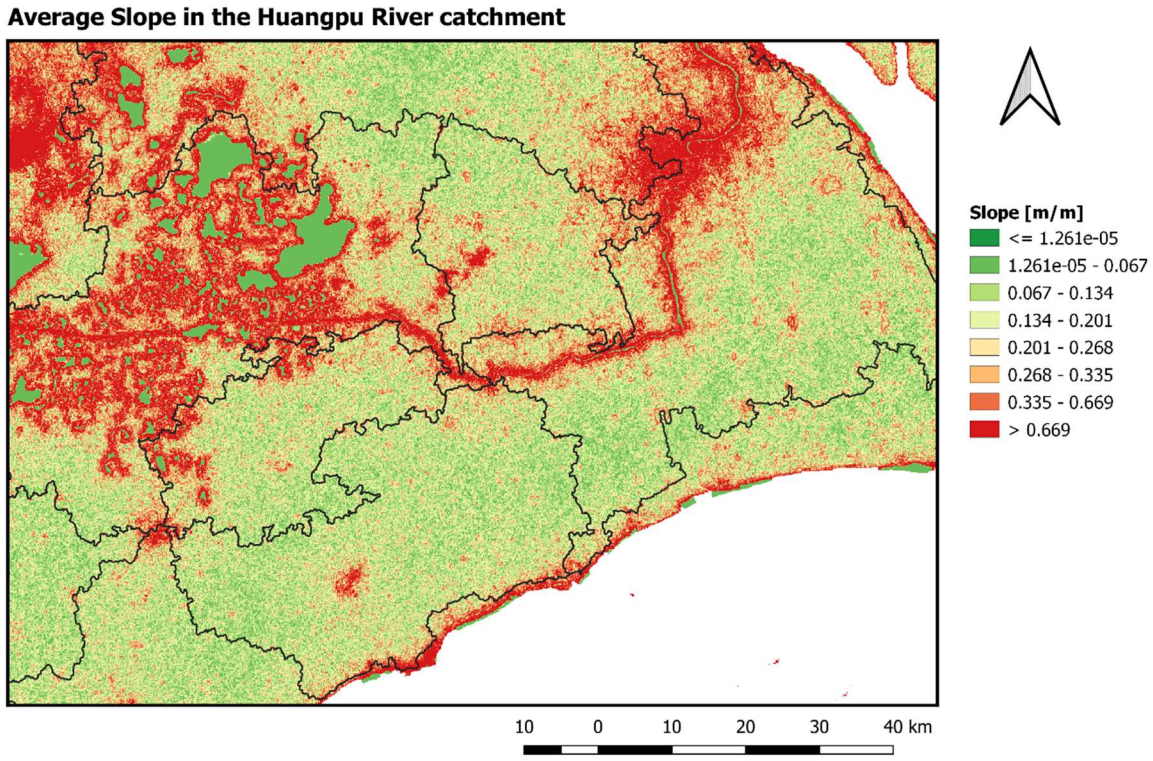

Fig 7. Average slope in the Huangpu River catchment

Regarding the dominant land use of the region, the datasets were obtained from the USGS – MODIS Land Cover Type product (MCD12Q1), produced annually at a 500 m resolution. A further simplification of the IGBP (International Geosphere Biosphere Program) scheme was also made as presented in Table 5, this allowed for the dataset to be used directly to estimate the corresponding runoff coefficient for each dominant land cover type.

Simplified class	**IGBP classes**
Forestland	Evergreen needleleaf forest, Evergreen broadleaf forest, Deciduous needleleaf forest, Deciduous broadleaf forest, Mixed forest, Closed shrublands, Open shrublands, Woody savannas
Grassland	Savannas, Grasslands
Cropland	Croplands, Cropland/Natural vegetation
Built-up land	Urban and built-up, Barren
Wetland / Water	Water, Permanent wetlands

Table 5. Land cover class simplification from IGBP scheme

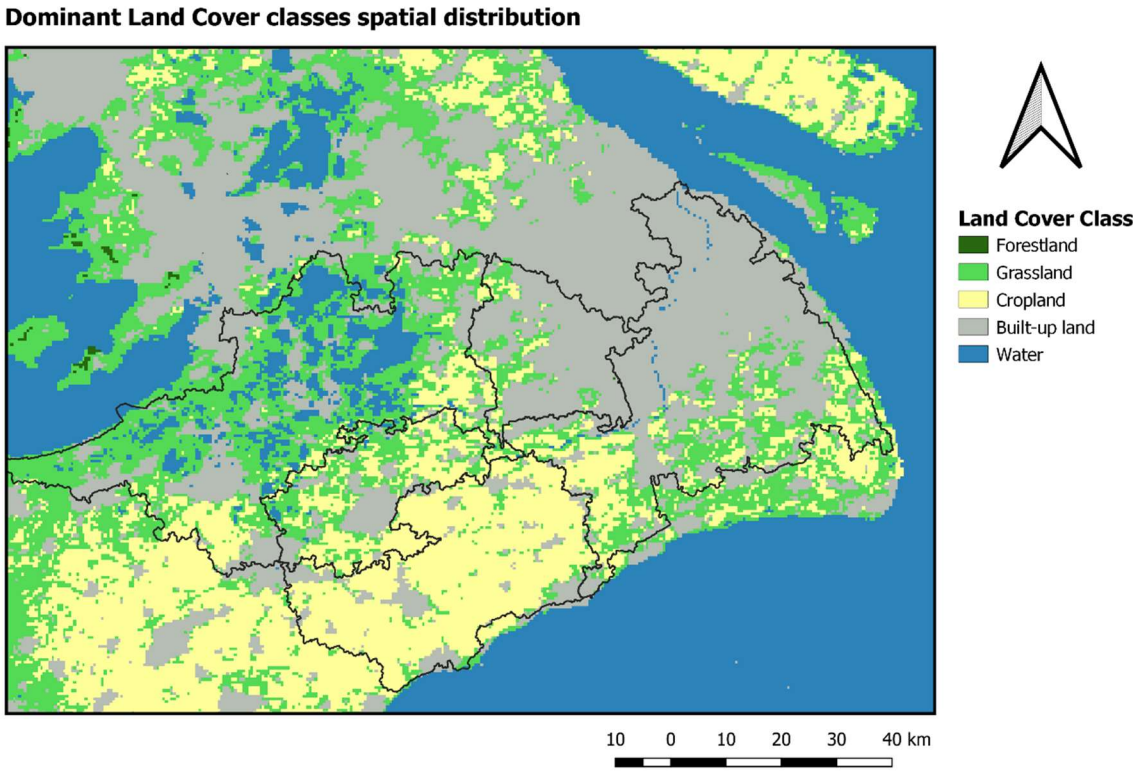

Fig 8. Dominant land cover classes in the Huangpu River catchment

Class \ Basin	Dianshan lake	Yuoxianjing	Damao	Youdungang	Huangpu river
Forestland	0.00%	0.00%	0.00%	0.03%	0.00%
Grassland	**44.83%**	**32.14%**	5.91%	13.92%	19.53%
Cropland	12.68%	**42.38%**	**79.66%**	7.74%	17.42%
Built-up land	22.58%	23.67%	14.40%	**78.31%**	**62.20%**
Water	**19.91%**	1.82%	0.04%	0.00%	0.85%

Table 6. Land cover percentages per basin

From this images, several conclusions can be made; first, the Dianshan lake basin not only has the highest percentage of water bodies coverage, but also due to the land's proximity to water it is mostly covered in grassland, the second least impervious surface after forestland, which also contributes to the hypothesis that the runoff contribution from rainfall in this area is mostly controlled by the outgoing discharge from Dianshan lake.

Below this basin is the Yuoxianding watershed, the most diverse of the 5, but ultimately dominated by cropland just as the Damao basin south of it, from which the largest contribution to discharge in the upstream portion of the Huangpu river can be expected. Finally both the Youdungang and Huangpu river basin are mostly covered by nearly impervious urban area, logical due to their proximity to Shanghai city.

To estimate the soil type corresponding to each raster cell, its soil content was analyzed using the sand, silt and clay content maps from the International Soil Reference and Information Centre (ISRIC) database at 250 m resolution (Hengl et al., 2017). These were combined using Table 7 as extracted from literature values from the USDA (Karamage et al., 2017) to determine the corresponding soil texture type for each grid cell.

Soil Texture Name	Sand	Silt	Clay
Sandy soil	85–100	0–15	0–10
Loamy sand	70–90	0–30	0–15
Sandy loam	43–80	0–50	0–20
Loam	23–52	28–50	7–27
Silt loam	0–50	50–88	0–27
Silt	0–20	88–100	0–12
Sandy clay loam	45–80	0–28	20–35
Clay loam	20–45	15–53	27–40
Silty clay loam	0–20	40–73	27–40
Sandy clay	45–65	0–20	35–45
Silty clay	0–20	40–60	40–60
Clay	0–45	0–40	40–100

Table 7. Soil type classes according to soil content percentages (Karamage et al., 2017)

Soil type \ Basin	Dianshan lake	Yuoxianjing	Damao	Youdungang	Huangpu river
Loam	1.04%	0.09%	0.19%	0.00%	0.04%
Silt loam	22.88%	**83.82%**	**94.88%**	**98.92%**	**97.54%**
Clay loam	4.75%	0.14%	0.16%	0.00%	0.24%
Silty clay loam	**71.33%**	15.94%	4.76%	1.08%	2.18%

Table 8. Soil type percentages per basin

From the combination of the sand, silt and clay content rasters, the resulting soil type was predominantly silty loam for 4 of the 5 basins, except for the Dianshan lake basin were silty clay loam was the most present one.

To combine all the datasets (slope, land use and soil content), the rasters were aligned and set to the resolution of the DEM – Slope map using the nearest neighbor interpolation method, the resulting map as presented in Figure 9 encompasses the assigned runoff coefficients for each cell following the values found in literature as described in Table 3. Due to the soil content datasets having no data for the water bodies, the runoff coefficient spatial distribution in Figure 9 shows these as no data values as well, the correction is made while processing the data considering that all rainfall that falls into water becomes direct runoff. Also, consistent with the values presented in Table 3, the highest values of the runoff coefficient are found in the most impervious urban areas on the north side of the Huangpu river basin, where the majority of the city of Shanghai concentrates.

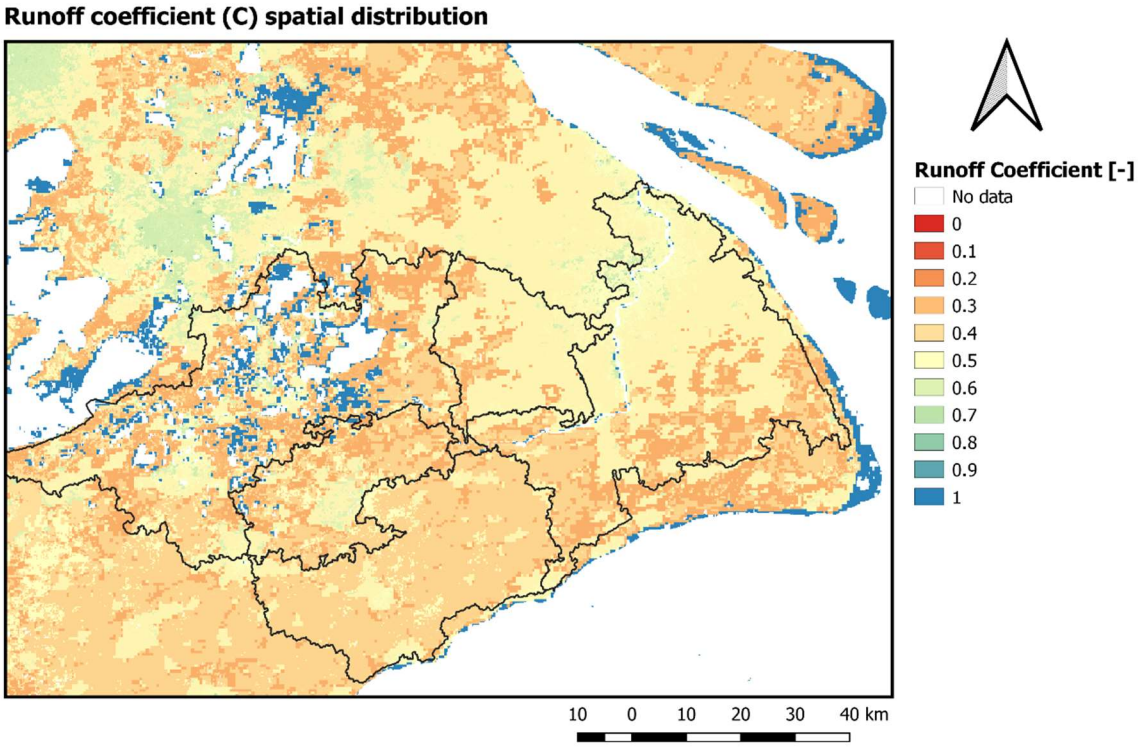

Fig 9. Runoff coefficient spatial distribution

Finally, to estimate the runoff consequent of the torrential rainfall that occurred during typhoon Fitow on each of the catchments, the precipitation data from the Global Precipitation Mission (GPM) was used to analyze the spatial distribution of the rainfall throughout the event in each of the catchments (Huffman, et al., 2019). Although the resolution of the data is quite coarse at 0.1 ° (approximately 11.1 km around the equator) when compared to the area of the catchments, the resulting rainfall intensity for the tropical storm event coincides to the descriptions of it, exceeding the 300 mm/day even in the outer areas of Shanghai (Bao et al., 2015). The corresponding maximum discharges for each area were calculated using the average intensity throughout the duration of the storm, taking into account the spatial distribution of the rainfall observed in the datasets, these results are presented in Table 9 after performing the calculations with the Rational Method equation.

Basin	Sub-basin	C [-]	i [mm/hr]	Σ Area [km^2]	Q [m^3/s]
Yuoxianjing	1	0.396	4.32	174.9	83.10
	2	0.392	3.75	121.8	49.87
	3	0.438	4.37	114.0	60.64
	4	0.377	3.80	162.3	64.64
	5	0.363	4.20	135.2	57.30
Damao	1	0.386	4.76	405.2	207.21
	2	0.400	5.15	131.7	75.38
	3	0.378	5.17	200.7	109.06
	4	0.395	4.89	153.6	82.51
	5	0.379	5.19	395.1	216.02
Youdungang (east)	1	0.482	3.17	57.8	24.55
	2	0.461	3.43	178.2	78.37
	3	0.438	3.16	178.0	68.55
	4	0.396	3.41	65.4	24.54
Youdungang (south)	5	0.401	3.45	108.0	41.53

Table 9. Peak discharges estimates for each sub-basin during typhoon Fitow

II.2.2 Time of concentration

To get a better representation of the time of response of the catchment to rainfall the time of concentration can be estimated, this refers to the time needed for water to flow from the furthest point in a watershed to its outlet, following the path along which the longest travel time is likely to occur. As with any empirical method, there are many formulas to estimate the time of concentration, each developed for a specific type of catchment in a certain type of region. Due to the large size of the basins, the formula developed by Passini was selected as the most adequate for this model (Salimi, Nohegar, Malekian, Hoseini & Holisaz, 2016).

$$Tc = 6.48(AL)^{0.333}S^{-0.5}$$

Where: A = basin area [km^2]

L = length of main channel [km]

S = average slope of the basin [m/m]

The length of the main channel was calculated as the longest flow path length for each of the sub-basins, the resulting times of concentration for each is presented in Table 10.

Basin	Sub-basin	LFP [km]	S [m/m]	TC - Passini [min]
Yuoxianjing	1	29.7	0.188	258
	2	27.8	0.376	158
	3	31.1	0.147	257
	4	24.0	0.295	187
	5	19.8	0.205	198
Damao	1	34.3	0.148	404
	2	42.3	0.214	248
	3	39.5	0.277	245
	4	37.9	0.151	299
	5	51.5	0.155	448
Youdungang (east)	1	23.5	0.310	129
	2	31.1	0.194	260
	3	21.3	0.243	204
	4	25.9	0.166	189
Youdungang (south)	5	34.0	0.391	159

Table 10. Time concentration estimates for each sub-basin using Passini's formula

II.3 Travel time

To finally be able to translate these results into discharge time-series that can be used as input for a DFM river model, the travel time of each peak discharge was calculated using Manning's equation for open channel flow to estimate the corresponding flow velocity and with it, the total travel time.

$$V = \frac{1}{n} \cdot {R_h}^{2/3} \cdot S^{0.5}$$

Where n is Manning's roughness coefficient, R_h is the channel's hydraulic radius, approximated by the channel depth for high width to depth ratios, and S is the channel slope.

Figure 10 represents the longest flow path streams used to estimate the time of concentration from the previous step, using it as a reference, travel time can be defined for sub-basin **1** as the time it takes its peak discharge to travel from point **A** to point **B**. The length and slope of this path can easily be estimated with the available information with QGIS tools, the Manning coefficient n as well considering the land use dataset mentioned earlier, the depth however is not readily available, varies with discharge and has a significant impact on the resulting travel times.

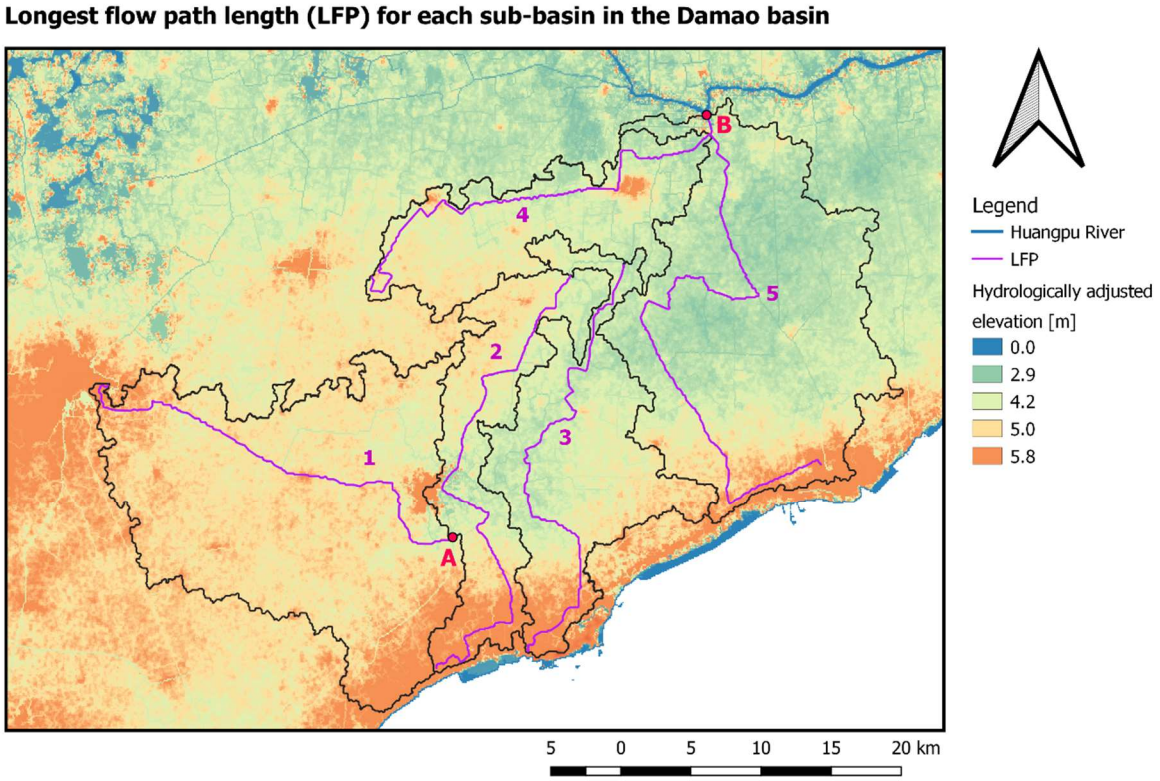

Figure 10. Longest flow path length for Damao sub-basins

(Andreadis, Schumann & Pavelsky, 2013) developed a near-global database of bank-full width and depths, along with their confidence intervals based on hydraulic geometry equations and the HydroSHEDS hydrography dataset. In their work, they mention a previously developed power law relationship between river width and depth and discharge:

$$w = 7.2\ Q^{0.50\pm0.02}(2.6 - 20.2)$$

$$d = 0.27\ Q^{0.30\pm0.01}(0.12 - 0.63)$$

Where the values in parenthesis represent the confidence intervals for the coefficients. Since the basin channels are mostly found outside of the Shanghai area and the dimensions needed to estimate the travel times are not available, by using the Google Maps engine to obtain the corresponding average river width at each reach throughout the sub-basins, a discharge related to that width was calculated and by adding the peak discharge estimated for the storm the corresponding depth was estimated as well, this depth was then compared to the values on the database developed by (Andreadis, Schumann & Pavelsky, 2013) to ensure it fit in the assigned confidence intervals for the stream in question. The resulting travel times along with the values used for its calculations in each basin are presented in Appendix A.

II.4 Discharge time-series

By adding the resulting travel times to the related time of concentration for each sub-basin, discharge time-series were generated for each basin as presented in Figures 11-14, these were extended for the entire storm duration of 51 hours (3,060 min) starting on October 6th, 2013 at 12:00 p.m.

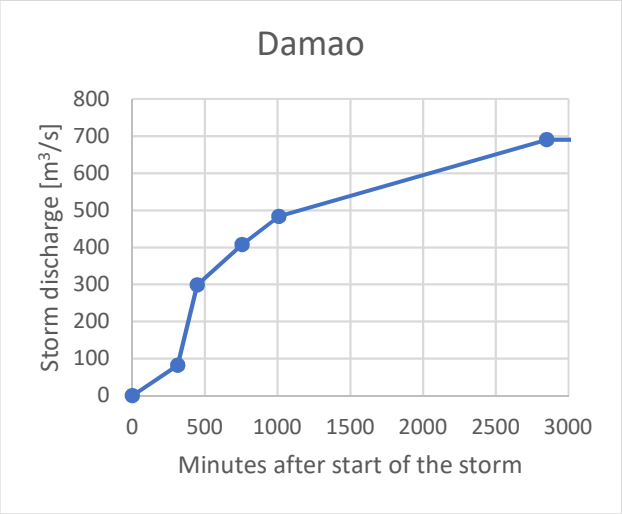

Figure 11. Discharge time-series Damao

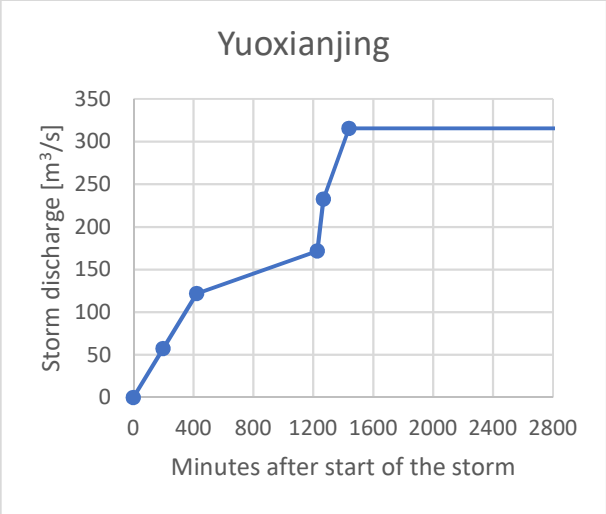

Figure 12. Discharge time-series Yuoxianjing

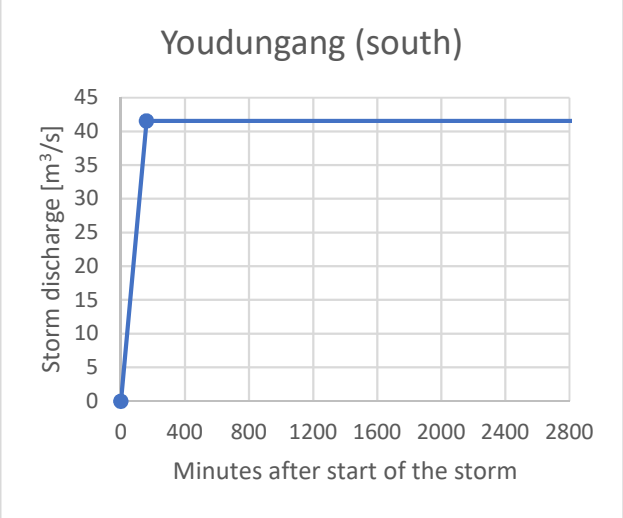

Figure 13. Discharge time-series Youdungang (south)

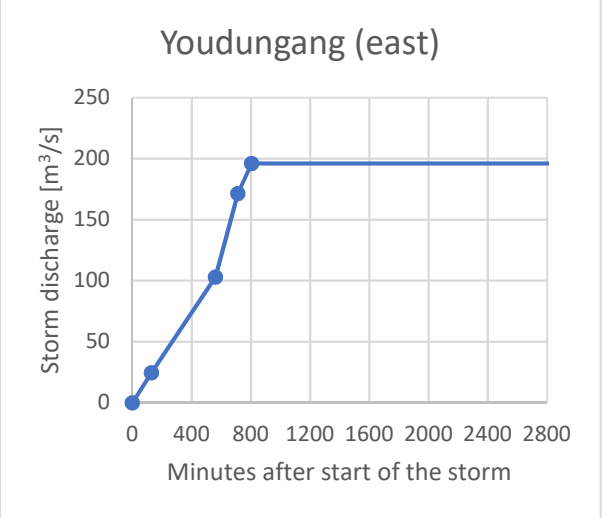

Figure 14. Discharge time-series Youdungang (east)

For the Dianshan lake basin, the resulting discharge time-series from two scenarios were considered; in the first one, only the precipitation that fell directly onto Dianshan lake was considered for storm runoff contribution, this was easily calculated with QGIS tools by creating a polygon that covered the lake area and then using the precipitation datasets from the storm to see how much had fallen within the lake, the second scenario considers not only this discharge, but also the one generated by the rainfall in the rest of the basin by assuming it is all being pumped out of the ponds and into Dianshan lake, this means that all rainfall that fall directly on water bodies becomes runoff, and for the other areas it is first multiplied by its corresponding runoff coefficient (similarly to how it was done in Section II.2) and then because the

time of concentration would vary too much between all the different water bodies, and it probably still wouldn't be accurate enough, it will be assumed conservatively that 70% of this runoff reaches the water bodies within 24 hours of the start of the storm. With this in mind, Figures 15 and 16 present the time-series of the additional discharge generated by the storm on the southward outlet of Dianshan lake (see Fig. 5) with and without pumping. The same Figures apply to the eastward outlet of Dianshan lake, only considering the discharge distribution to be 83% south, 17% east (Xiong et al., 2017).

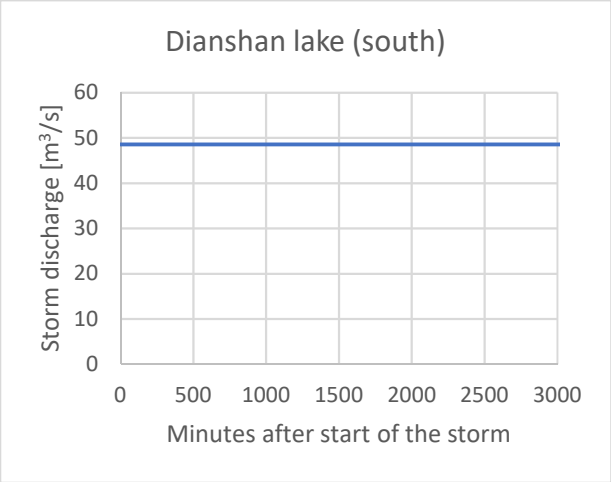

Figure 15. Discharge time-series without pumping

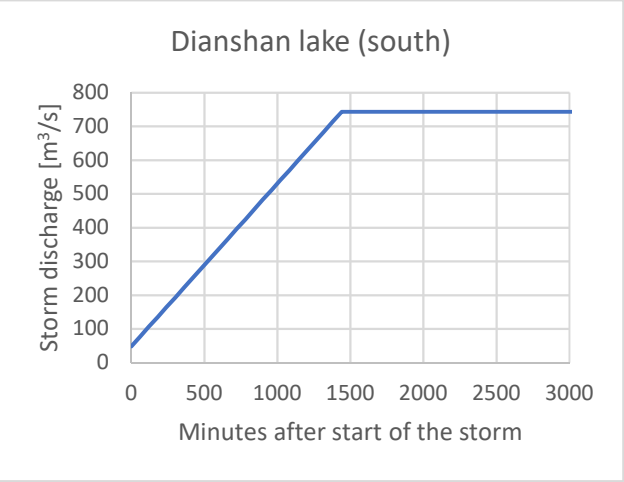

Figure 16. Discharge time-series with pumping

II.5 D-Flow Flexible Mesh – River model

D-Flow Flexible Mesh (DFM) is a software module within Delft3D in development by Deltares, it is able to perform hydrodynamical simulations via the use of numerical solutions to the shallow water equations (Navier-Stokes), based on unstructured grids (Deltares, 2018). The RFDGRID tool is used within this software to develop said grids, the one used on this particular model was developed by previous studies on this same area, and the simulations carried out on it will serve as a further contribution to this research. The grid was readily checked on orthogonality and smoothness, as presented in Appendix B. Similarly, the bathymetry for this model was already available, as were the corresponding calibrated roughness coefficients for each section of the river as presented in Table 11.

Section	Roughness coefficient
River mouth – Huangpu Park	0.013
Huangpu Park – Mishidu	0.030
Mishidu – Lakes	0.060

Table 11. Roughness coefficients for DFM – River model

A set of boundary conditions was also needed to model the state of the river water level, on the downstream location in the river mouth, the measured water level was selected to account for the storm surge that occurred during the typhoon event, while on upstream locations the discharge measured in the Taipu canal just downstream of Taihu lake was used to account for the period before the flood gate was closed, as well as a constant discharge of 200 m^3/s as calibrated by previous studies to account for the incoming steady discharge before the storm from the many tributaries to the Huangpu river. The

model was set with a start time at 03/Oct/2013 00:00 and end time at 09/Oct/2013 00:00, with a time step of 5 minutes, and an initial water level of 3 meters.

The two main observation points were selected as depicted by Figure 5 in the location of the hydrological stations Huangpu Park (midstream) and Mishidu (upstream) to be able to compare the model results with the measurements during that time period. Finally, the discharge corresponding to the rainfall – runoff estimated from the hydrological model were set as Sources in the DFM – River model, the corresponding discharge time-series to each basin is further explained in Section III.1 and can be seen as small red arrows in the model representation in Figure 17.

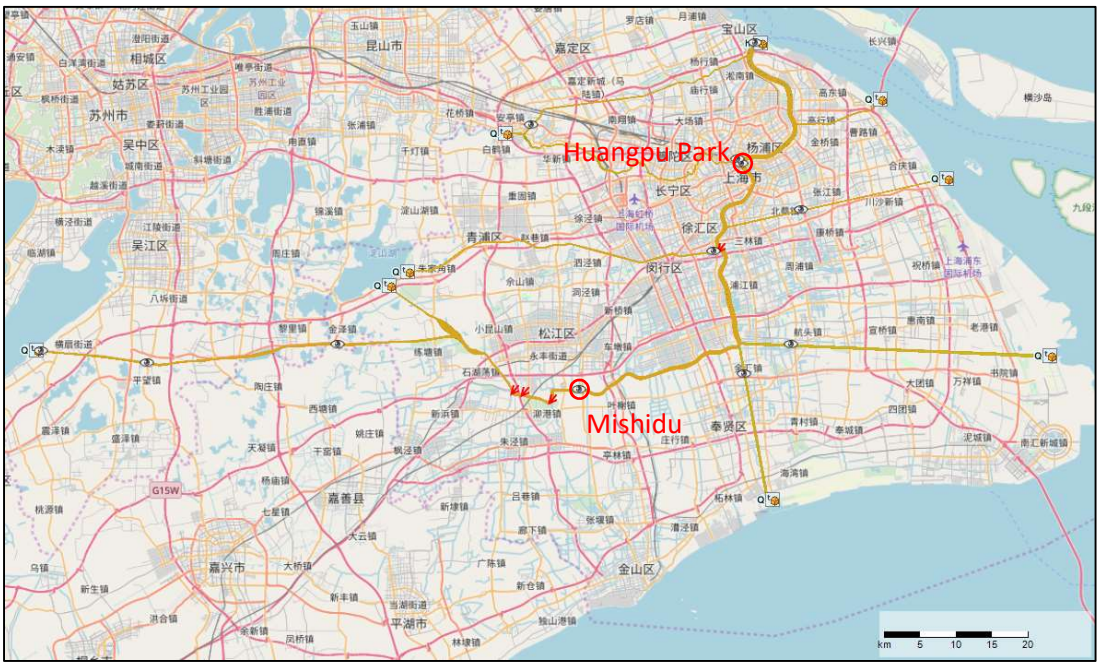

Figure 17. DFM – River model visual representation

The resulting plots for the water levels with the calibrated values, without any additional discharge from rainfall is presented for both stations in Figures 18 and 19.

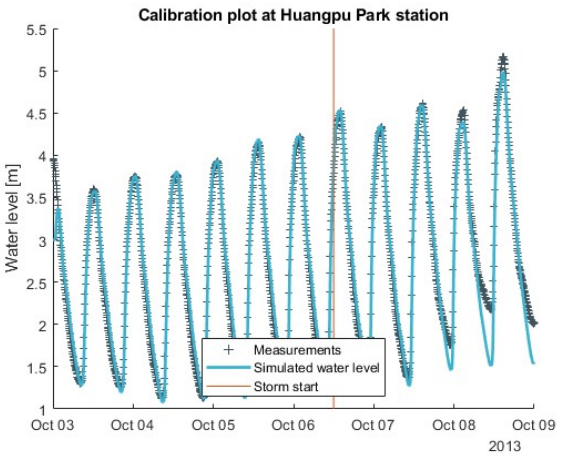

Figure 18. Calibration plot at Huangpu Park

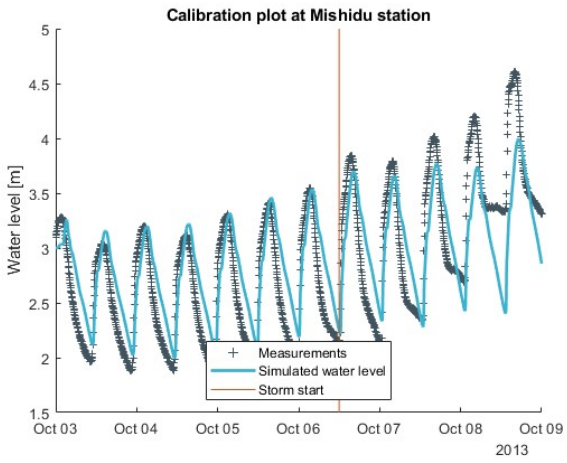

Figure 19. Calibration plot at Mishidu

III. Results

III.1 Scenarios

To analyze the overall contribution of rainfall to runoff from the watersheds, a set of different plausible combinations is proposed considering the existing water gates described in Figure 5. This allows for the observation of the behavior of the water level along the Huangpu river, during the period of the tropical storm Fitow in October 2013, given different scenarios as described in Table 12. The main focus will be water level observed at the upstream Mishidu hydrological station (location depicted in Figures 5 and 17) as during this storm the highest recorded water level at this station was observed, this will allow for a comparison with the measurements during the event, as well as comparison with the scenario without flow contribution presented in Figure 19. The second point of focus is the water level observed at the Huangpu Park hydrological station further downstream closer to the river mouth, as a means to ensure the calibration of the river model, however since the water levels at this station are mostly controlled by the tide there is very little variation in the predictions by the model regardless of the scenario (Ke et al., 2018), the resulting water level plots at this station can be found in Appendix C.

Scenario \ Gate	A	B	C	D	Pumping	Contributing Basins
1	Open	Closed	Closed	Closed	No	Damao
2	Closed	Open	Closed	Closed	No	Yuoxianjing, Youdungang (south)
3	Closed	Closed	Closed	Open	No	Dianshan lake (east), Youdungang (east)
4	Open	Open	Closed	Closed	No	Damao, Yuoxianjing, Youdungang (south)
5	Closed	Open	Open	Closed	No	Dianshan lake (south), Taihu lake, Yuoxianjing, Youdungang (south)
6	Closed	Open	Open	Closed	Yes	Dianshan lake (south), Taihu lake, Yuoxianjing, Youdungang (south)
7	Open	Open	Closed	Open	No	Damao, Yuoxianjing, Youdungang (both), Dianshan lake (east)
8	Closed	Open	Open	Open	No	Dianshan lake (both), Taihu lake, Yuoxianjing, Youdungang (both)
9	Closed	Open	Open	Open	Yes	Dianshan lake (both), Taihu lake, Yuoxianjing, Youdungang (both)
10	Open	Open	Open	Open	No	All
Worst-case	Open	Open	Open	Open	Yes	All

Table 12. Scenarios for DFM river model

III.1.1 Scenarios 1 – 3

The first three scenarios give way to analyze the response of the river system to the incoming discharge of each individual basin:

- Scenario 1 (Figure 20) represents the response to runoff from the Damao watershed, this is the largest of the basins and the one that contributes the most by far, even just with this basin the model is already approaching the maximum water level height measured, and is a fair representation of the peaks observed throughout the storm.
- Scenario 2 (Figure 21) is about the Yuoxianjing basin and a small portion of Youdungang basin, from the upstream areas these are the ones that contribute the least, yet the model predicts the peaks observed in the first 2 days of the storm (October 6 and 7) quite well, this may suggest that the response of the system is slower than expected, and that the times of concentration calculated in Section II.2.2 are smaller than in reality.
- Scenario 3 (Figure 22) only considers the discharge going directly into the more downstream portions of the river, which is made evident by the clear underestimation of the water level by the model as soon as the storm begins, as rainfall contribution to the upstream areas is being neglected.

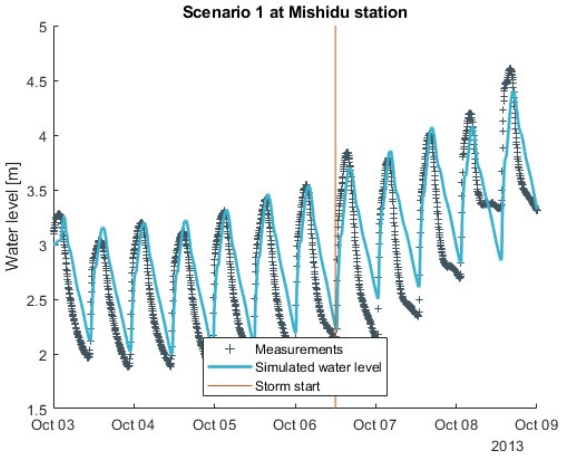

Figure 20. Scenario 1 at Mishidu

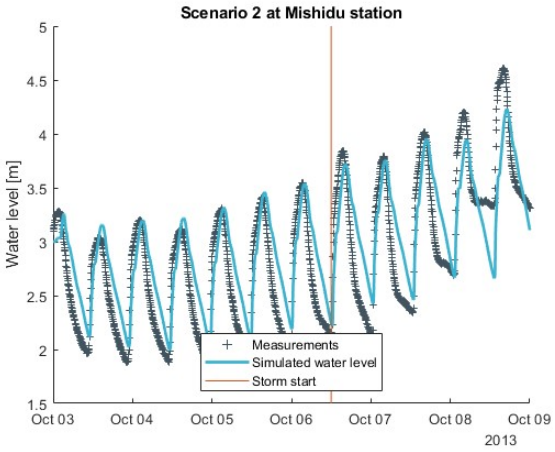

Figure 21. Scenario 2 at Mishidu

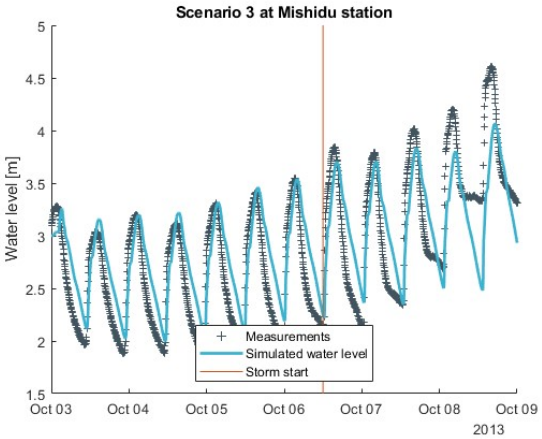

Figure 22. Scenario 3 at Mishidu

III.1.2 Scenarios 4 – 9

Scenarios 4 – 9 aim to analyze the system's response to the different plausible scenarios occurring when it is assumed that Gate B is open. Scenarios 4 – 6 show the different possibilities while assuming Gate D on the eastern side is closed, while Scenarios 7 – 9 show the same combinations but considering Gate D open. For this reason Scenarios 4 and 7, 5 and 8, and 6 and 9, are presented together, since the latter represent the slight increase in the water level caused by the higher amount of runoff in the system, even when this is directed straight to the more downstream section, due to the tide dominant character of the river this changes are still observed upstream.

- Scenarios 4 and 7 (Figures 23 and 24) analyze the response of the system to the contribution of the upstream basins without any additional discharge from Dianshan lake. These scenarios model the peaks of the storm on the later stages of the typhoon quite well, but tend to overestimate on the earlier stages, indicating that while the runoff contribution from rainfall is quite accurate, it takes longer for it to enter the system than what it was estimated, similar to what was observed in Scenario 2.
- Scenario 5 and 8 (Figures 25 and 26) model the water levels assuming the runoff incoming from the Damao basin is retained at its water gate. The early stages of the storm fit almost perfectly with the measurements at this station, however on the later stages it fails to reach not only the maximum values observed at the peak, but also underestimates the troughs by predicting much smaller water levels.
- Scenario 6 and 9 (Figures 27 and 28) do the same as scenarios 5 and 8, but this time under the assumption that the precipitation falling in the Dianshan lake basin is being pumped into the system. The results are comparable to the ones obtained in Scenarios 4 and 7, only the overestimation of the peaks is greater, even in the earlier stages, this can be adjudged to the fact that the storage capacity of the lake and the water bodies might not be accurately represented, and the system in reality awaits for this capacity to be exhausted before starting to pump the water out.

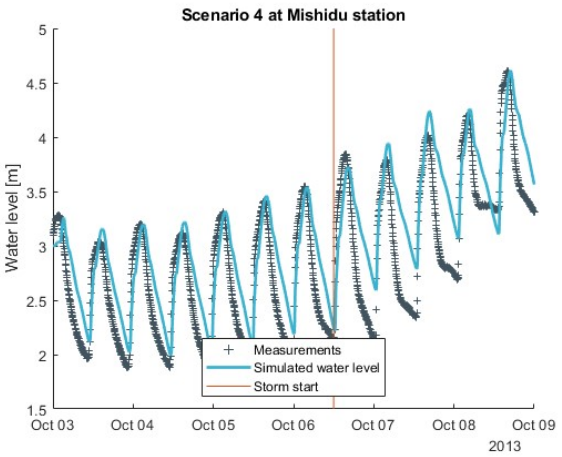

Figure 23. Scenario 4 at Mishidu

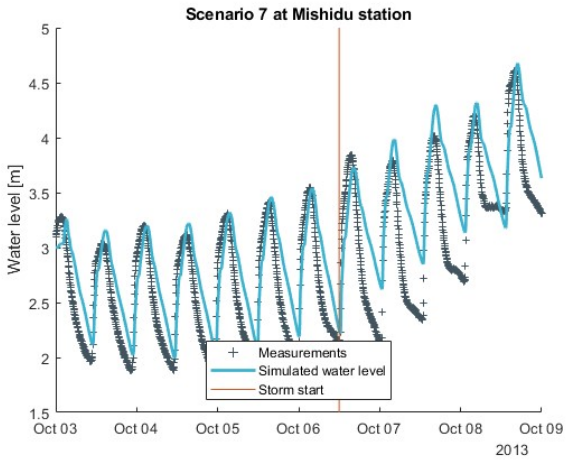

Figure 24. Scenario 7 at Mishidu

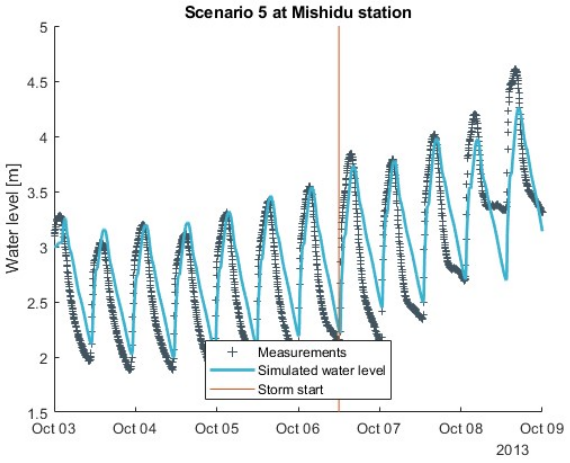

Figure 25. Scenario 5 at Mishidu

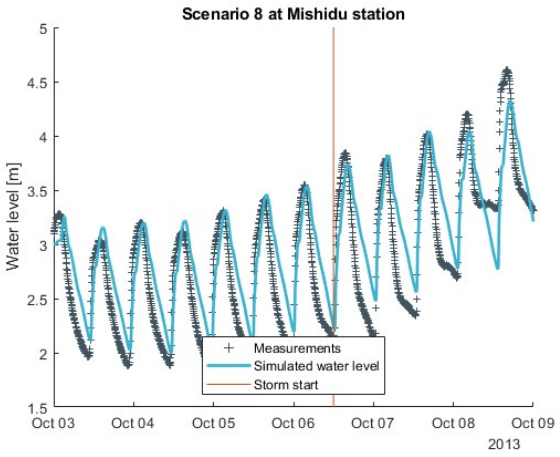

Figure 26. Scenario 8 at Mishidu

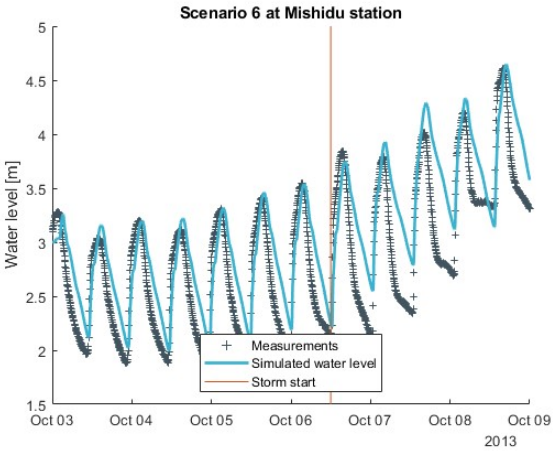

Figure 27. Scenario 6 at Mishidu

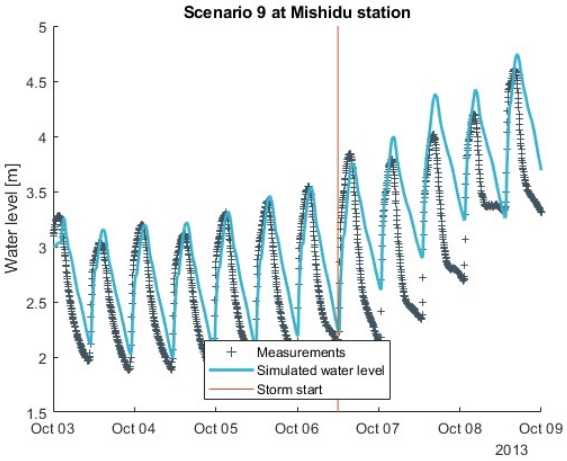

Figure 28. Scenario 9 at Mishidu

III.1.3 Scenarios 10 and 11 (worst-case)

These two scenarios represent the response of the river system without any restrains from water gates, both without (Scenario 10) and with (Scenario 11) pumping of the runoff in the Dianshan lake basin.

- Scenario 10 encompasses the most logical combination of events, and while the errors observed in previous Scenarios (4 and 7) are repeated, the slight overestimation of the water level goes hand in hand with the tendency of the Rational method to overestimate discharge values, and unlike Scenario 11, it actually provides a good estimate of what the maximum observed values during the storm where.
- Scenario 11 is clearly overestimating the discharge from the start of the storm in a very unrealistic manner, meaning that during this event either the water incoming from the Damao basin was stopped before it joined the river, or that the water in the Dianshan lake basin wasn't pumped into the system.

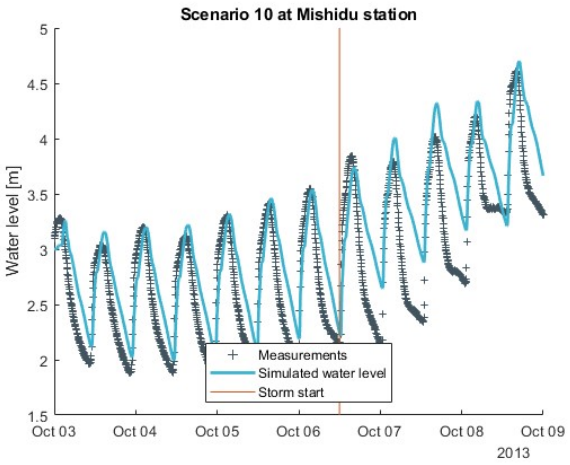

Figure 29. Scenario 10 at Mishidu

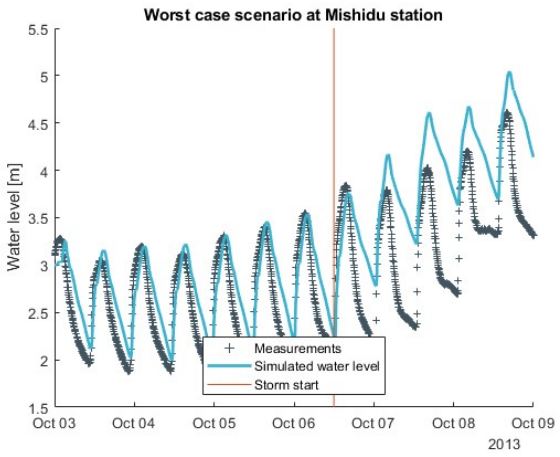

Figure 30. Worst-case scenario at Mishidu

III.2 Typhoon Haikui

In order to assess the performance of the hydrological model on different conditions, the runoff coefficients estimated for each area in section II.2.1 were used along with the precipitation data observed during Typhoon Haikui downloaded from the GPM database to estimate the corresponding peak discharges to this rainfall event, building afterwards the corresponding discharge time-series for this event following a similar procedure as in section II.4, considering in this case a storm starting August 7th, 2012 at 6:00 a.m. These time-series were used as input on the DFM-river model as sources, together with the discharge measured at the Taipu canal just downstream of Taihu lake flood gate and the water level measured at the river mouth during this period as boundary conditions, the values used as input for this model are presented in Appendix D. The resulting modelled water level at the Mishidu and Huangpu Park hydrological stations is presented in Figures 31-34.

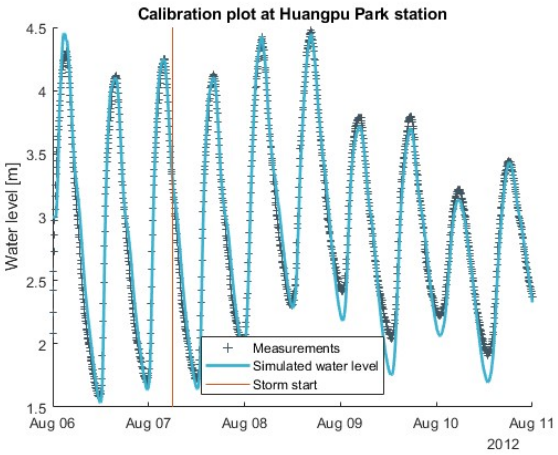

Figure 31. Calibration plot at Huangpu Park

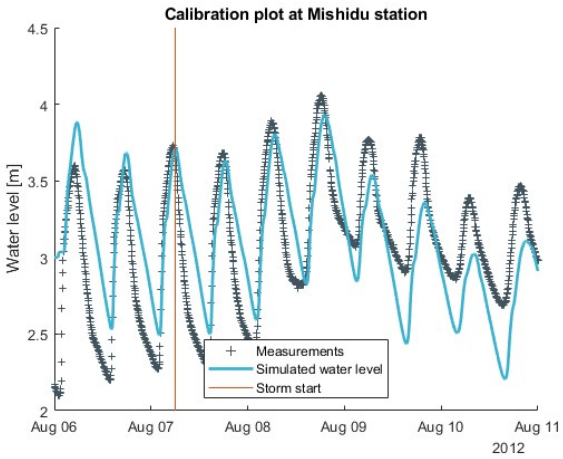

Figure 32. Calibration plot at Mishidu

Figures 31 and 32 represent the model results without the additional discharge generated by runoff, again the model is able to represent the measurements at the midstream station in Huangpu Park, due to the

strong dominance of tide in this section of the river, whereas in the more upstream areas at Mishidu station the water levels are notably underestimated on the later stages of the storm event.

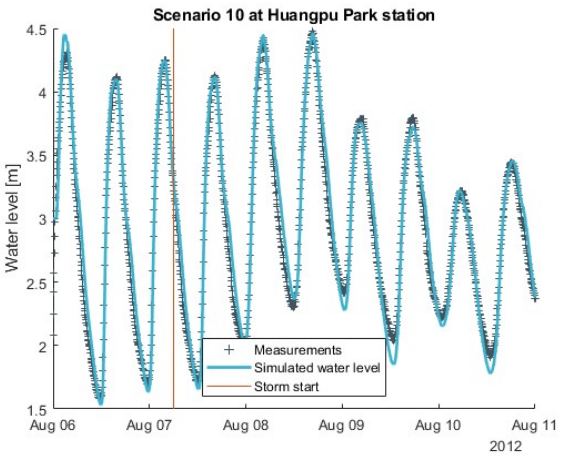

Figure 33. Scenario 10 at Huangpu Park

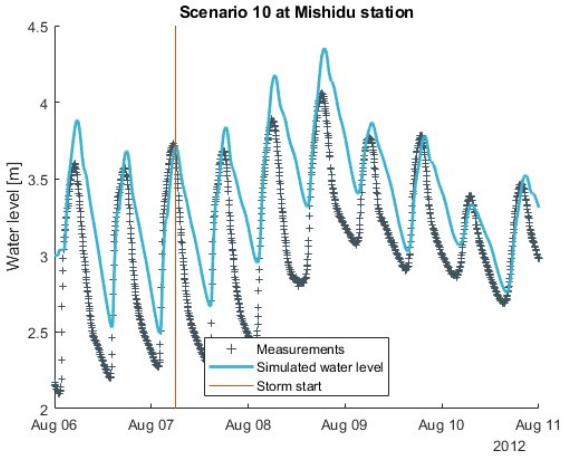

Figure 34. Scenario 10 at Mishidu

Figures 33 and 34 represent the model water level predictions using the discharge time-series derived for typhoon Haikui, following the system settings described for scenario 10 in Table 12. Again there is little influence of the discharge on the water levels at the midstream station, although the water levels at low tide seemed to be predicted slightly better. For the upstream station however, the addition of the runoff generated by rainfall again corrects quite accurately the water level rise at the later stages of the storm, on the early stages of the storm on the other hand, it is overestimating the measured values, which is indicative that the response of the system was slower than predicted by the hydrological model.

III.3 River profile

To get a better picture of the flood risk represented by the modelled water levels, a comparison was made between the predicted maximum water level along the river and the estimated embankment height. For the first of these two, the results given by Scenario 10 were selected, as it is representative of the situation where all the basins are contributing to the observed water levels, and still within range of the measurements (unlike the results from Scenario 11). The embankment height was obtained from measurements made in 2008 and due to land subsidence and renovations might not be as accurate on this day. These are presented together in Figure 35.

The proximity of the maximum water level to the embankment height near the Mishidu hydrological station just further highlights the flood risk related to torrential precipitation events, especially when taking into account the rainfall – runoff contribution from the upstream areas. It can also be seen along the river, that there are several spots with relatively low height, which translate into higher flood risk for the area, meaning that the overall safety of the embankment is notably lower in some areas than the 1000-year return period design.

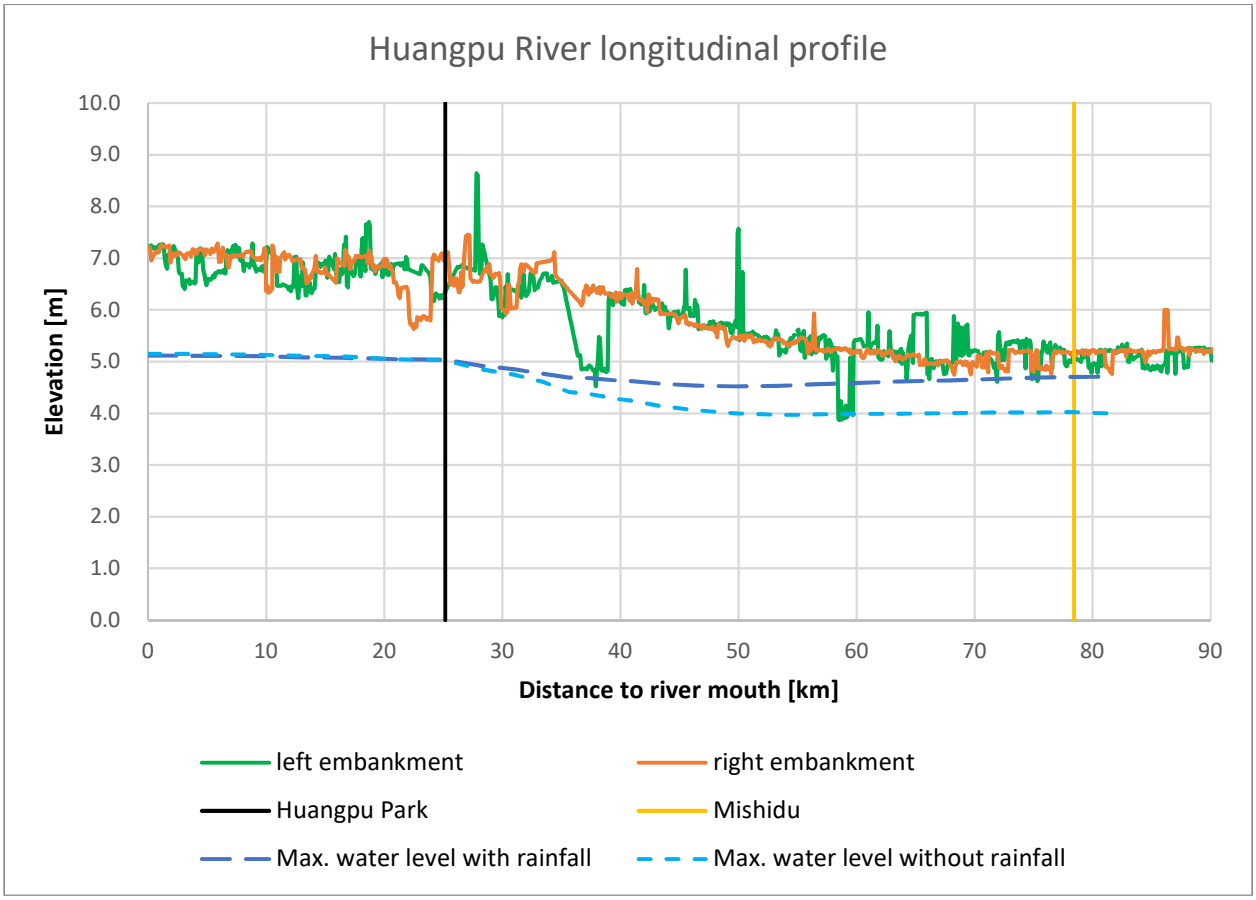

Figure 35. Huangpu River longitudinal profile

The light blue dashed line in Figure 35 shows the maximum predicted water levels along the river without taking into account the contribution by rainfall, evidencing the importance and impact of precipitation in the water levels of the upstream areas, raising the maximum water level over 0.7 meters in the stretches furthest from the river mouth. It is also clear that barely any changes are perceived in the downstream areas, as the lines coincide at the Huangpu Park hydrological station, which goes hand in hand with the results obtained from the model at this station with all different scenarios (Appendix C).

IV Conclusion

The aim of this research project was to assess the impact of torrential rainfall during tropical storms on the water levels along the Huangpu River in Shanghai, this was done by creating a hydrological model of the river, outlining the different contributing watersheds, studying their hydrological regime, and analyzing the processes that controlled the rainfall-runoff relation in each of them, identifying unique characteristics such as the mild slope along the catchments that causes them to have a relatively slow response to rainfall, or the irregular flow paths caused either by the flatness of the slope or by the high presence of water bodies, especially in the upstream area north of the Taipu canal. Based on these basin characteristics, the rational method was used to estimate the peak discharges in each of the region corresponding to the torrential rainfall experience during typhoon Fitow in October 2013, these were later translated into discharge time-series to serve as input in a numerical model of the river water levels built in Delft 3D's D-Flow Flexible Mesh, with which several scenarios could be modelled and later compared to the measurements during the storm event, the hydrological model was then validated by comparing the results with the same parameters for a different storm, typhoon Haikui in August 2012. Finally the scenario that presented the best model predictions was selected to get an estimate of the maximum water level at different points along the river, which was then compared to the measurements of the existing flood defenses to assess the flood risk related to the rainfall event.

The problems encountered throughout this research project were mostly related to the complex topography of the region and the consequent need of high-resolution data to produce reliable results. This also meant that for the most part conventional methods for hydrological modeling could not be employed, especially in the upstream region where the surface is covered by ponds and lakes that affect significantly the response of the system to rainfall events. Another example of this is seen in the Youdungang basin, where due to the densely urbanized area on the eastern side of it, the hydrologically adjusted elevation from the MERIT datasets forces the flow direction to the opposite side by missing the connection between the stream that crosses the basin from Dianshan lake to the Huangpu river, this is graphically depicted in the map in Appendix E. Although this situation was solved by correcting the direction of the flow in the hydrological model, it definitely highlights the uncertainties brought by the resolution of the datasets.

To conclude, the results found in this research project showcase the relevance of rainfall induced runoff during typhoon events, by presenting a simple hydrological model that encompasses the processes and land characteristics that regulate the hydrological regime of the region, and later using a hydrodynamic model that assesses the behavior of the river system under various plausible scenarios, which can later be compared to the current safety conditions for a full flood defense safety assessment. At the same time, the results found in the hydrodynamic model of the river with the addition of rainfall induced runoff, present a significant improvement for the water level simulations in the late stages of typhoon events, there is however, an area of improvement on the simulations for the early stages of typhoon events as the model tends to underestimate the time of response of the system to rainfall events.

Finally, it calls for future studies to analyze rainfall contribution not only to runoff but also to urban flooding via a high-resolution urban model of Shanghai city, as well as bringing out the importance of a combined river and coastal flood model of the region, capable of predicting the hydraulic loads related to the different potential flood defense failure mechanisms and with which the co-occurrence of several flood scenarios can be assessed.

References

Andreadis, K., Schumann, G., & Pavelsky, T. (2013). A simple global river bankfull width and depth database. *Water Resources Research*, *49*(10), 7164-7168. doi: 10.1002/wrcr.20440

Bao, X., Davidson, N., Yu, H., Hankinson, M., Sun, Z., & Rikus, L. et al. (2015). Diagnostics for an Extreme Rain Event near Shanghai during the Landfall of Typhoon Fitow (2013). *Monthly Weather Review*, *143*(9), 3377-3405. doi: 10.1175/mwr-d-14-00241.1

Deltares (2018). D-Flow Flexible Mesh - (User Manual). Deltares.

Fumin, R., Gleason, B., & Easterling, D. (2002). Typhoon impacts on china's precipitation during 1957-1996. *Advances In Atmospheric Sciences*, *19*(5), 943-952. doi: 10.1007/s00376-002-0057-1

Hengl, T., Mendes de Jesus, J., Heuvelink, G., Ruiperez Gonzalez, M., Kilibarda, M., & Blagotić, A. et al. (2017). SoilGrids250m: Global gridded soil information based on machine learning. *PLOS ONE*, *12*(2), e0169748. doi: 10.1371/journal.pone.0169748

Huffman, G.J., E.F. Stocker, D.T. Bolvin, E.J. Nelkin, Jackson Tan (2019), GPM IMERG Final Precipitation L3 1 month 0.1 degree x 0.1 degree V06, Greenbelt, MD, Goddard Earth Sciences Data and Information Services Center (GES DISC), Accessed: November 8th, 2019, 10.5067/GPM/IMERG/3B-MONTH/06

Ke, Q., Jonkman, S., van Gelder, P., & Bricker, J. (2018). Frequency Analysis of Storm-Surge-Induced Flooding for the Huangpu River in Shanghai, China. *Journal Of Marine Science And Engineering*, *6*(2), 70. doi: 10.3390/jmse6020070

Kwast, H., Menke, K., & Sherman, G. (2019). *QGIS for Hydrological Applications*.

Lauriat, G. (2019). AJOT's Top 100 Containerports A to Z. Retrieved 25 September 2019, from https://www.ajot.com/premium/ajot-ajots-top-100-containerports-a-to-z/P0

Liu, Y., Zhou, Y., Ju, W., Chen, J., Wang, S., & He, H. et al. (2013). Evapotranspiration and water yield over China's landmass from 2000 to 2010. *Hydrology And Earth System Sciences*, *17*(12), 4957-4980. doi: 10.5194/hess-17-4957-2013

Lyu, H., Shen, S., Yang, J., & Yin, Z. (2019). Scenario-based inundation analysis of metro systems: a case study in Shanghai. *Hydrology And Earth System Sciences Discussions*, 1-30. doi: 10.5194/hess-2019-28

Mihalik, E., Levine, N., & Amatya, D. (2008). Rainfall-Runoff Modeling of the Chapel Branch Creek Watershed using GIS-based Rational and SCS-CN Methods. *2008 Providence, Rhode Island, June 29 - July 2, 2008*. doi: 10.13031/2013.25084

Salimi, E., Nohegar, A., Malekian, A., Hoseini, M., & Holisaz, A. (2016). Estimating time of concentration in large watersheds. *Paddy And Water Environment*, *15*(1), 123-132. doi: 10.1007/s10333-016-0534-2

Sulla-Menashe, D., Friedl, M. (2018). User Guide to Collection 6 MODIS Land Cover (MCD12Q1 and MCD12C1) Product

"Urban Storm Water Management Manual For Malaysia" (2000) Department of Irrigation and Drainage Malaysia. Percetakan Nasional Malaysia Berhad.

Wei, Y., & Leung, C. (2005). Development Zones, Foreign Investment, and Global City Formation in Shanghai*. *Growth And Change*, *36*(1), 16-40. doi: 10.1111/j.1468-2257.2005.00265.x

Xiong, G., Wang, G., Wang, D., Yang, W., Chen, Y., & Chen, Z. (2017). Spatio-Temporal Distribution of Total Nitrogen and Phosphorus in Dianshan Lake, China: The External Loading and Self-Purification Capability. *Sustainability*, *9*(4), 500. doi: 10.3390/su9040500

Yamazaki, D., Ikeshima, D., Tawatari, R., Yamaguchi, T., O'Loughlin, F., & Neal, J. et al. (2017). A high-accuracy map of global terrain elevations. *Geophysical Research Letters*, *44*(11), 5844-5853. doi: 10.1002/2017gl072874

Yang, L., Wang, L., Li, X., & Gao, J. (2019). On the Flood Peak Distributions over China. *Hydrology And Earth System Sciences Discussions*, 1-34. doi: 10.5194/hess-2019-322

Yin, J., Yu, D., Yin, Z., Wang, J., & Xu, S. (2012). Multiple scenario analyses of Huangpu River flooding using a 1D/2D coupled flood inundation model. *Natural Hazards*, *66*(2), 577-589. doi: 10.1007/s11069-012-0501-1

Zhang, H., Liu, S., Ye, J., & Yeh, P. (2017). Model simulations of potential contribution of the proposed Huangpu Gate to flood control in the Lake Taihu basin of China. *Hydrology And Earth System Sciences*, *21*(10), 5339-5355. doi: 10.5194/hess-21-5339-2017

Zhou, Z., Liu, S., Zhong, G., & Cai, Y. (2017). Flood Disaster and Flood Control Measurements in Shanghai. *Natural Hazards Review*, *18*(1), B5016001. doi: 10.1061/(asce)nh.1527-6996.0000213

Appendix A

Channel dimensions used for travel time estimations

Basin	Sub-basin	River width [m]	Path length [km]	Path slope	Depth* [m]	Travel time [min]
Yuoxianjing	1	71	9.81	8.16E-05	1.91	235.44
	2	111	16.19	2.47E-05	1.48	837.60
	3	111	16.19	2.47E-05	1.63	784.85
	4	150	11.59	1.29E-04	1.74	234.68
Damao	1	65	24.17	1.24E-05	1.48	1763.21
	2	81	4.59	2.18E-05	1.33	271.72
	3	97	13.12	4.57E-05	1.48	497.78
	4	130	1.65	7.90E-04	1.64	14.04
Youdungang (east)	1	56	11.81	1.35E-04	1.19	301.90
	2	61	7.82	1.02E-04	1.19	229.38
	3	63	4.16	1.20E-04	1.08	120.43

** Depth varies with discharge, and so does the resulting travel time, the values presented in this table are calculated with the initial values, for the accumulated travel times the increase in depth due to accumulated discharge was also taken into account.*

Appendix B

Grid orthogonality and smoothness check

Orthogonality

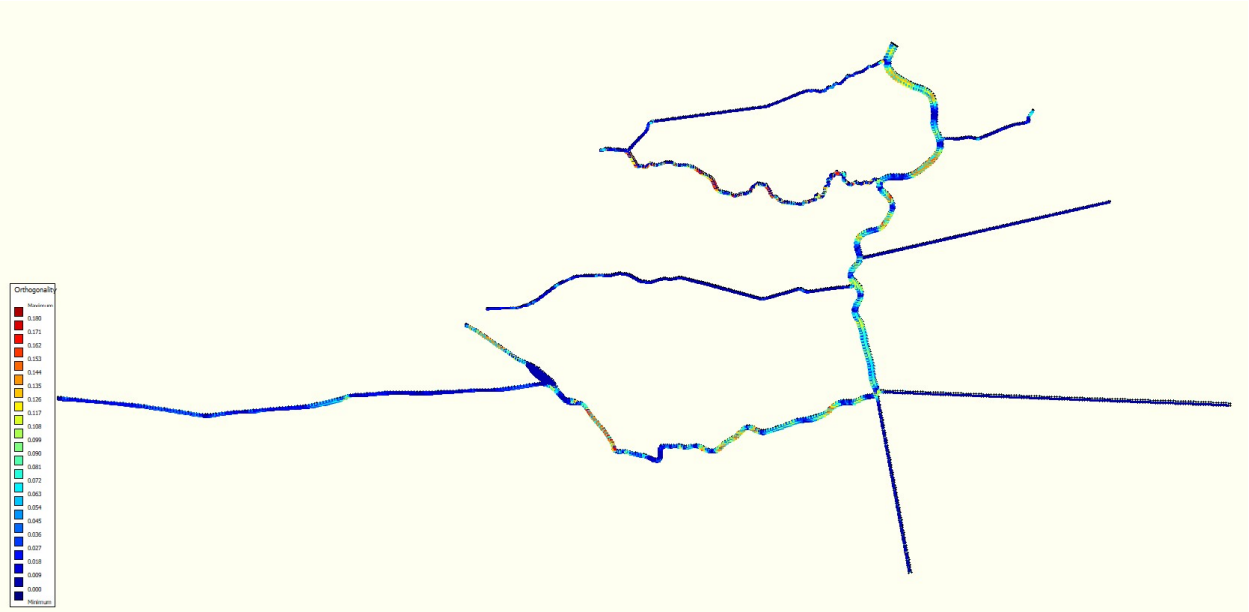

Smoothness

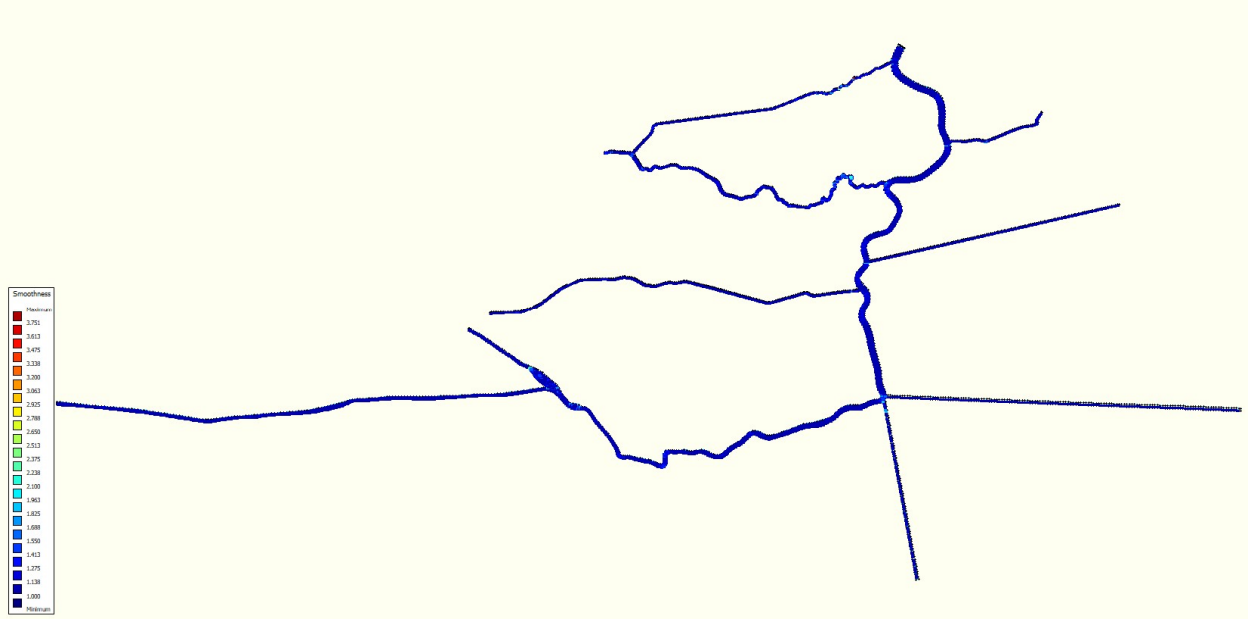

Appendix C

Scenarios at Huangpu Park hydrological station

Scenarios 1 – 3:

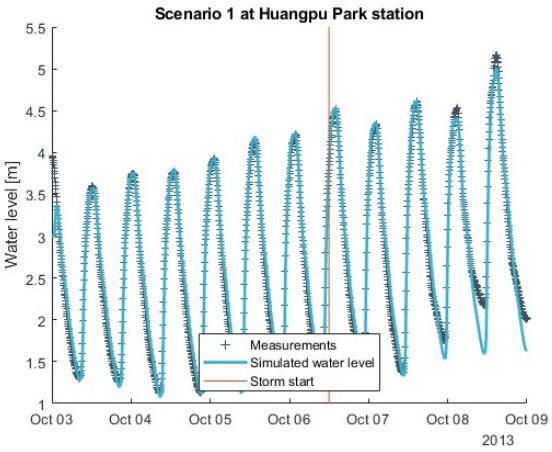

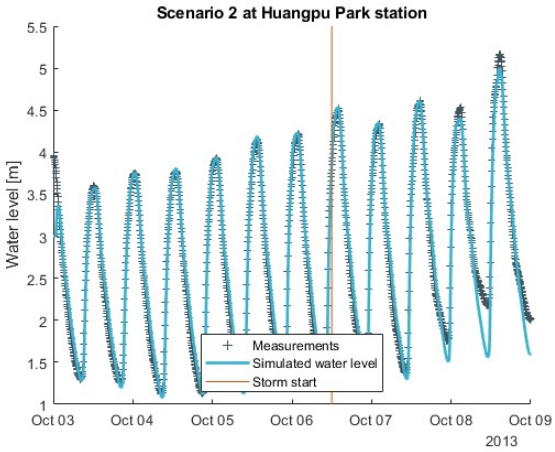

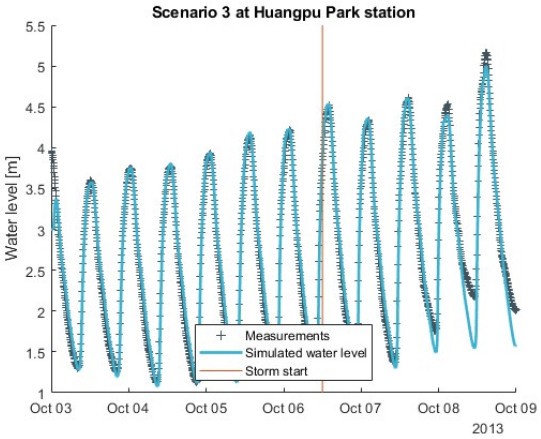

Scenarios 4 – 9:

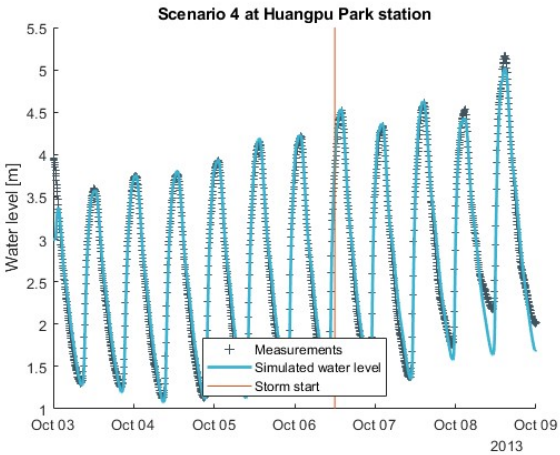

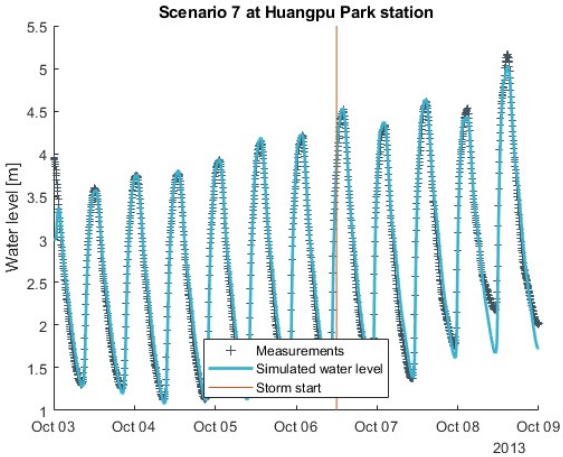

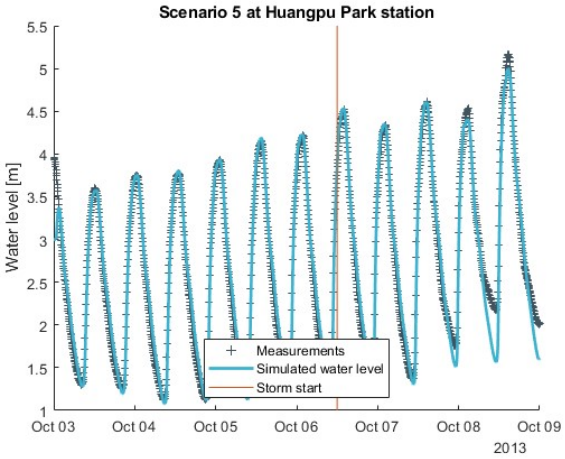

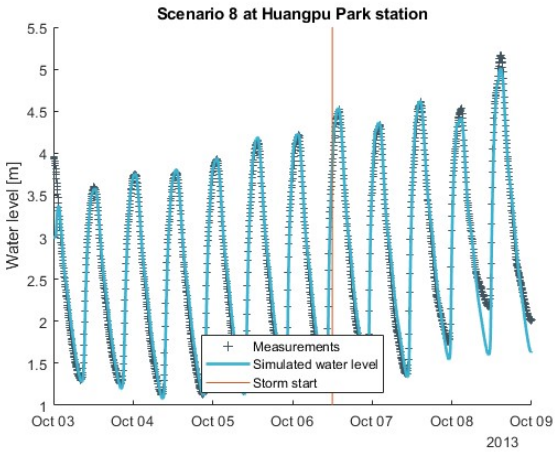

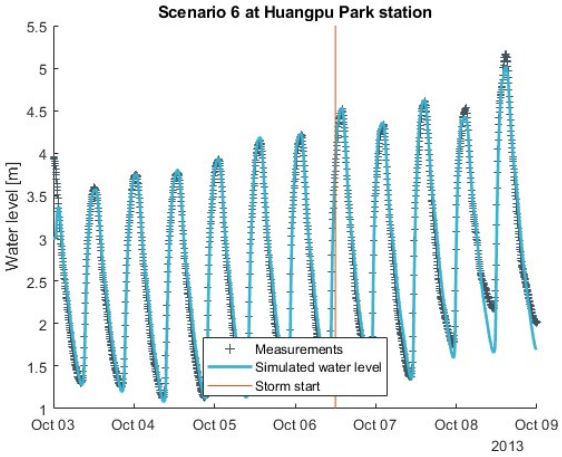

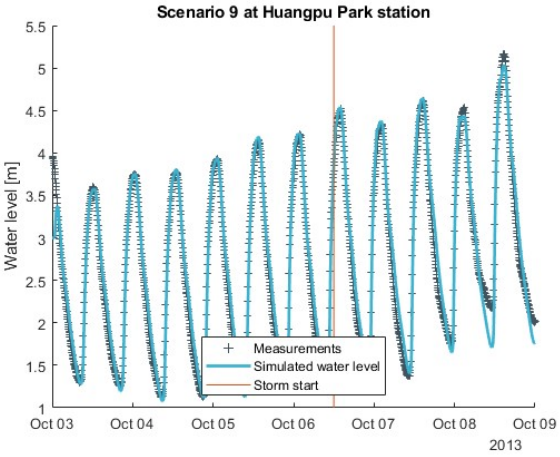

Scenarios 10 – 11:

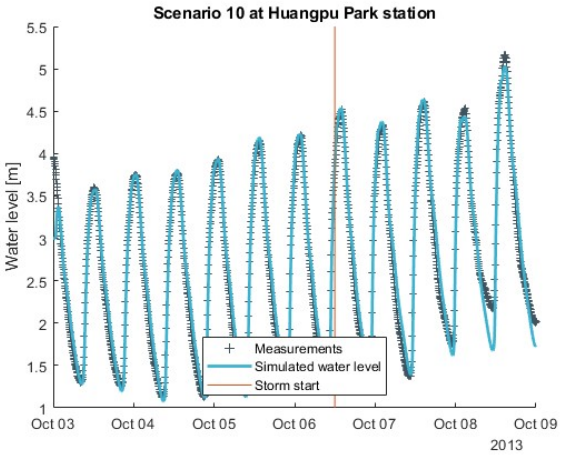

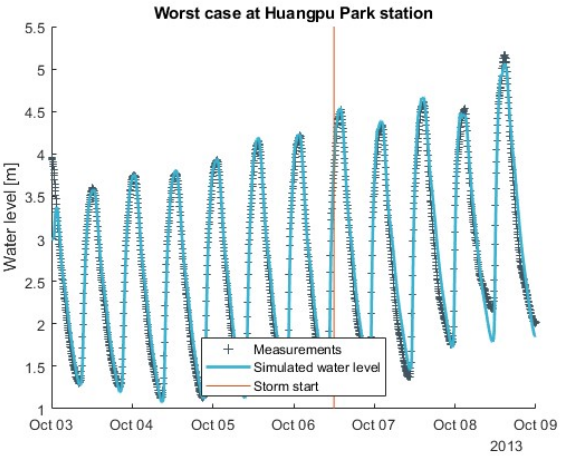

Appendix D

Peak runoff values per basin estimated for typhoon Haikui

Basin	Sub-basin	C [-]	i [mm/hr]	A [km^2]	k	Q [m^3/s]
Yuoxianjing	1	0.396	4.320	174.866	0.278	83.104
	2	0.392	3.752	121.841	0.278	49.874
	3	0.438	4.368	114.015	0.278	60.643
	4	0.377	3.804	162.342	0.278	64.640
	5	0.363	4.199	135.200	0.278	57.300
Damao	1	0.386	3.501	405.19	0.278	152.25
	2	0.400	3.798	131.69	0.278	55.63
	3	0.378	3.999	200.71	0.278	84.41
	4	0.395	3.538	153.61	0.278	59.75
	5	0.379	4.011	395.07	0.278	166.89
Youdungang (east)	1	0.482	3.168	57.83	0.278	24.553
	2	0.461	3.428	178.25	0.278	78.367
	3	0.438	3.161	178.03	0.278	68.550
	4	0.396	3.407	65.35	0.278	24.539
Youdungang (south)	5	0.401	3.450	107.97	0.278	41.534

DFM – River model inputs for typhoon Haikui

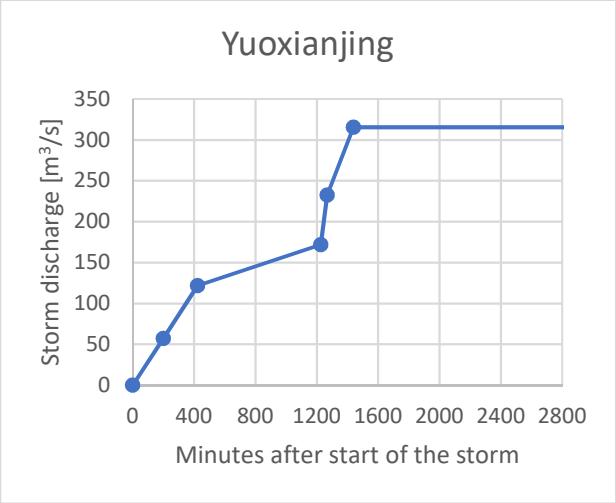

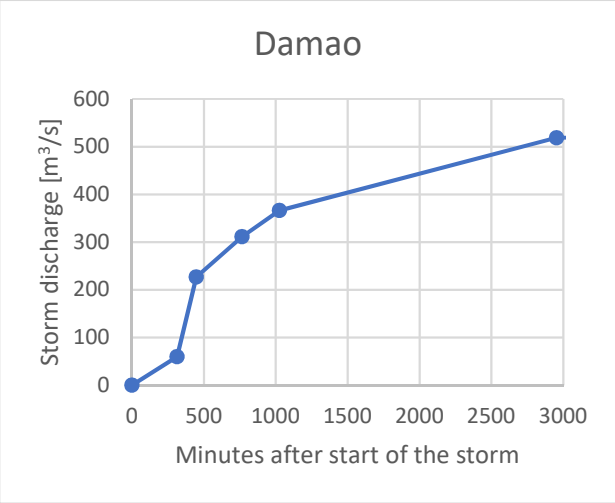

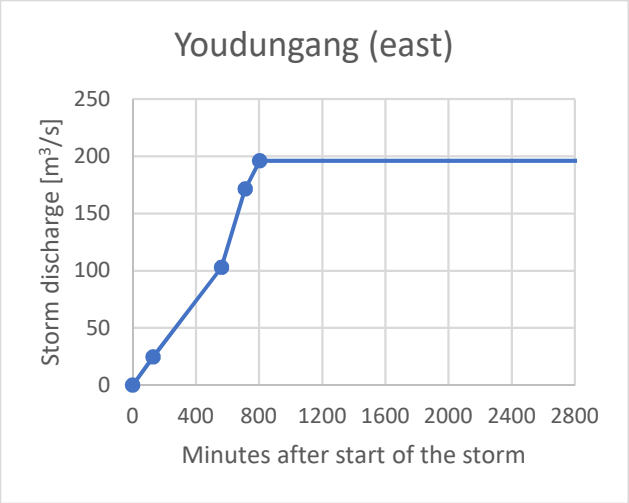
Youdungang (east)
Storm discharge [m3/s]
250
200
150
100
50
0
0
400
800
1200
1600
2000
2400
2800
Minutes after start of the storm

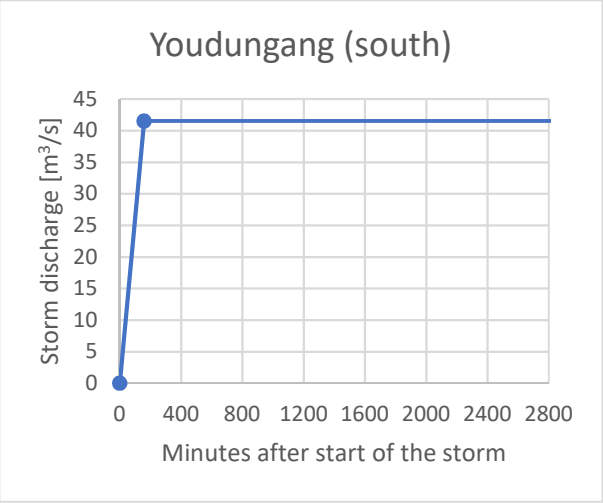
Youdungang (south)
Storm discharge [m3/s]
45
40
35
30
25
20
15
10
5
0
0
400
800
1200
1600
2000
2400
2800
Minutes after start of the storm

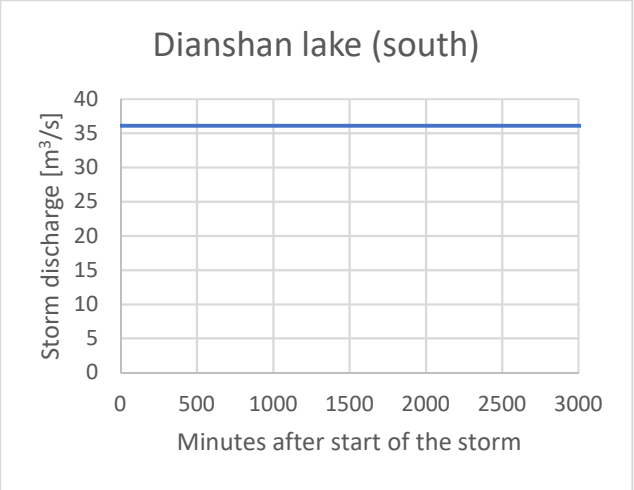
Dianshan lake (south)
Storm discharge [m3/s]
40
35
30
25
20
15
10
5
0
0
500
1000
1500
2000
2500
3000
Minutes after start of the storm

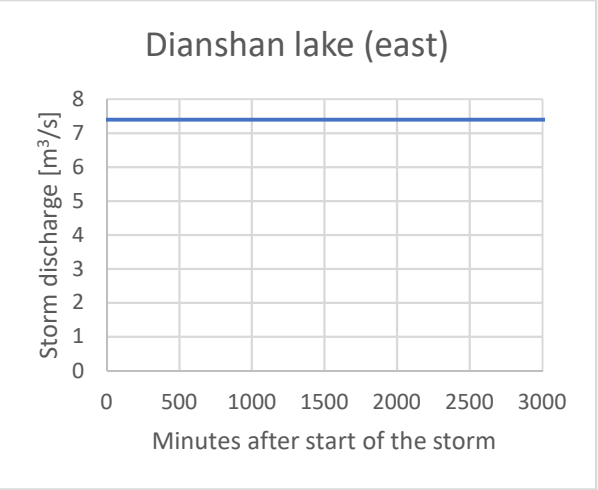
Dianshan lake (east)
Storm discharge [m3/s]
8
7
6
5
4
3
2
1
0
0
500
1000
1500
2000
2500
3000
Minutes after start of the storm

Appendix E

Youdungang basin hydrologically adjusted elevation